frontiers | Frontiers in Nanotechnology

REVIEW
published: 04 July 2022
doi: 10.3389/fnano.2022.940825

Emerging Memristive Devices for Brain-Inspired Computing and Artificial Perception

*Jingyu Wang, Ying Zhu, Li Zhu, Chunsheng Chen and Qing Wan**

School of Electronic Science and Engineering, Nanjing University, Nanjing, China

Brain-inspired computing is an emerging field that aims at building a compact and massively parallel architecture, to reduce power consumption in conventional Von Neumann Architecture. Recently, memristive devices have gained great attention due to their immense potential in implementing brain-inspired computing and perception. The conductance of a memristor can be modulated by a voltage pulse, enabling emulations of both essential synaptic and neuronal functions, which are considered as the important building blocks for artificial neural networks. As a result, it is critical to review recent developments of memristive devices in terms of neuromorphic computing and perception applications, waiting for new thoughts and breakthroughs. The device structures, operation mechanisms, and materials are introduced sequentially in this review; additionally, late advances in emergent neuromorphic computing and perception based on memristive devices are summed up. Finally, the challenges that memristive devices toward high-performance brain-inspired computing and perception are also briefly discussed. We believe that the advances and challenges will lead to significant advancements in artificial neural networks and intelligent humanoid robots.

Keywords: memristor, artificial synapse, artificial neural network, brain-inspired computing, bionic perception

OPEN ACCESS

Edited by:
Zhongrui Wang,
The University of Hong Kong, Hong Kong SAR, China

Reviewed by:
Bowen Zhu,
Westlake University, China
Hong Wang,
Xidian University, China

****Correspondence:***
Qing Wan
wanqing@nju.edu.cn

Specialty section:
This article was submitted to Nanodevices, a section of the journal Frontiers in Nanotechnology

Received: *10 May 2022*
Accepted: *25 May 2022*
Published: *04 July 2022*

Citation:
Wang J, Zhu Y, Zhu L, Chen C and Wan Q (2022) Emerging Memristive Devices for Brain-Inspired Computing and Artificial Perception. Front. Nanotechnol. 4:940825. doi: 10.3389/fnano.2022.940825

INTRODUCTION

Von Neumann Architecture and Brain-Inspired Computing

In recent decades, traditional computing architecture, aided by Moore's law, has fueled the technological revolution and ushered us into the information age. However, because computing and storage units are separated, the von Neumann bottleneck appeared (Backus, 1978), including low work efficiency, memory walls, high energy consumption, and power consumption walls (Theis and Wong, 2017; He et al., 2018; Huang et al., 2021). To address these issues, scientists turned their attention to the human brain and proposed brain-inspired computing (neuromorphic computing). The human brain is made up of approximately 10^{11} neurons and 10^{15} synapses (Neves et al., 2008). These neurons and synapses are organized in three dimensions to form a complex information processing neural network. In comparison to traditional computers, the human brain is a wholly parallel computing structure on a large scale, it relies on neurons and synapses to transmit and process received information for perception, learning, memory, thinking judgment, emotional expression, and problem-solving while consuming little energy and working efficiently. (Silver et al., 2016). Until now, researchers have developed a wide range of artificial neural networks (ANNs) based on

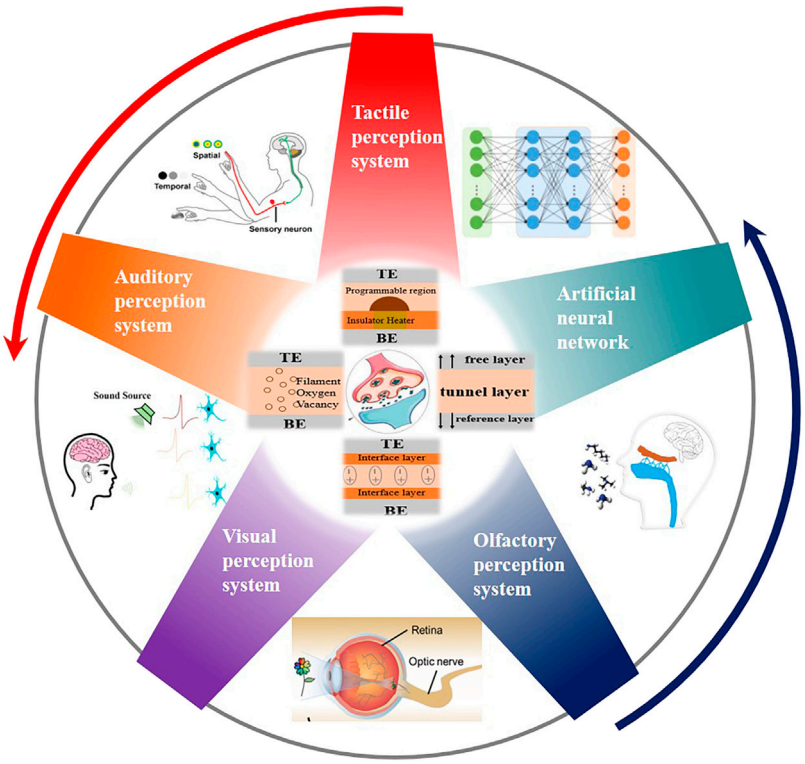

FIGURE 1 | An overview of memristive devices used for brain-inspired computing and perception systems [adapted from Wan et al. (2018), Xue et al. (2018), Guo L. et al. (2020), Wu et al. (2021)].

software and hardware with the goal of mimicking the computing power of the human brain (LeCun et al., 2015). Software-based artificial neural networks have performed well in image recognition natural language processing (Collobert and Weston, 2008; Hinton et al., 2012) and other tasks (Vinyals et al., 2019). However, software-based artificial neural networks consume considerable energy and space, and they cannot efficiently simulate the neural network's parallel processing mechanism (Markram, 2006). Recently, various electronic devices, including two-terminal and three-terminal artificial synapses, have been constructed to simulate synaptic behavior (Chang et al., 2011; Kuzum et al., 2012a; Wang et al., 2012b; Kim et al., 2013; Shi et al., 2013; Wan et al., 2014; Zhu et al., 2014; Mao et al., 2021). Two-terminal devices include memristors, phase change memory, atomic switch and so on. They have been widely used to mimic synaptic plasticity due to their simple structure, low power consumption, small physical volume, and ease of large-scale integration. However, it is difficult for them to perform signal transmission and self-learning functions at the same time. Ferroelectric synaptic transistors, double-layer synaptic transistors, electrochemical synaptic transistors, and photoelectric synaptic transistors are examples of three-terminal synaptic transistors. They have good stability, relatively controllable test parameters, and can perform signal transmission and self-learning simultaneously. However, the structure and mechanism are complex and difficult to use on a large scale in the short term. By integrating these artificial synapses with other devices and peripheral circuits, hardware-based artificial neural networks can be built, they are envisioned as powerful alternative computing systems currently (Cooper and Bear, 2012; Wang Q. et al., 2021).Memristors and memristive-related devices, as a kind of two-terminal device, have been widely used because of their simple structure, low power consumption, small physical volume and ease of large-scale integration, (Torrezan et al., 2011; Wang et al., 2012a; Pickett and Williams, 2012; Prezioso et al., 2015; Xu et al., 2016). In this review, we will concentrate on synaptic plasticity, memristive-related devices' structure and operation mechanisms and their applications in brain-inspired computing and perception **Figure 1**.

Synapses and Synaptic Plasticity

The entire behavior of the human brain is based on an extremely complex network consisted of neurons and synapses. Neurons are the most fundamental structural and functional units in the human brain for perception, information processing, and learning, artificial synapses and artificial neurons can memorize and integrate signals respectively, which are functional units in the human brain for perception, information processing, and learning. Learning and memory require the joint action of synapses and neurons. Neurons

collect, integrate and refine a large amount of sensory information, and dynamically modify the synaptic weight, so as to realize learning and memory. A neuron is made up of a cell body, axons,/dendrites. Two adjacent neurons are connected by synapses, by varying the connection strength (synaptic weight) between two neurons, the integration effect of biological synapses on signals can be altered. This is known as synaptic plasticity, all memory and learning are thought to be underpinned by it (Lynch et al., 1976; Malenka et al., 1999).The schematic diagram of neurons and synapse are shown in **Figure 2A**, synapse converts electrical signals into chemical signals, and then converted into electrical signals to transmit information between presynaptic neurons and postsynaptic neurons. Postsynaptic neurons respond in two ways: excitatory postsynaptic potential (EPSP) and inhibitory postsynaptic potential (IPSP). EPSP refers to the depolarization of the postsynaptic membrane potential caused by neurotransmitters, resulting in an increase in the neuron's excitability to other stimuli. IPSP is the membrane potential of the postsynaptic membrane caused by neurotransmitters, resulting in the neuron's reduced excitability to other stimuli. Synaptic plasticity is classified into two types: short-term plasticity (STP) and long-term plasticity (LTP), as shown in **Figure 2A**. STP returns to baseline levels quickly after synaptic activity (Boyn et al., 2017a), usually within tens of milliseconds to several minutes. Paired-pulse facilitation (PPF) is a type of STP in which the postsynaptic signal is amplified when the second input signal is the same as the first input signal. PPF can participate in some neuronal tasks, such as simple learning and information processing. Paired-pulse depression (PPD) refers to the inhibition of postsynaptic signals. LTP persists for seconds, minutes, or longer, depending on its biological intention (Guo et al., 2018), it refers to plastic changes that result in permanent changes to neural networks, allowing the brain to store vast amounts of information. There are currently two major types of synaptic learning rules. Hebbian learning is one of the most important theories, it compares a neuron's input and output information and updates the neuron's input weight parameters. The concept of spike-timing dependent plasticity (STDP) extends Hebb's theory, proving that synaptic weights can be influenced by the temporal relationship between presynaptic spikes and postsynaptic spikes. Furthermore, Bienenstock–Cooper–Munro (BCM) is another learning rule that takes into account frequency-dependent plasticity and sliding correction thresholds. The postsynaptic neuron outputs an integrated postsynaptic spike rate to each neuron according to the BCM learning rule (Caporale and Dan, 2008; Cooper and Bear, 2012; Wang Q. et al., 2021). Spike-rate-dependent plasticity (SRDP) indicate that high-frequency presynaptic pulses above a certain frequency threshold will induce synaptic plasticity and synaptic weights can be altered by varying the frequency of presynaptic pulses. Low frequency presynaptic pulses below a certain frequency threshold inhibit the response.

ARTIFICIAL MEMRISTIVE SYNAPSES AND OPERATION MECHANISMS

Memristor's appearance provides a new physical basis for the development of a new type of computing system with high energy efficiency and integration of storage and computing. It was first predicted by Leon O. Chua (Chua, 1971) and it is the fourth basic

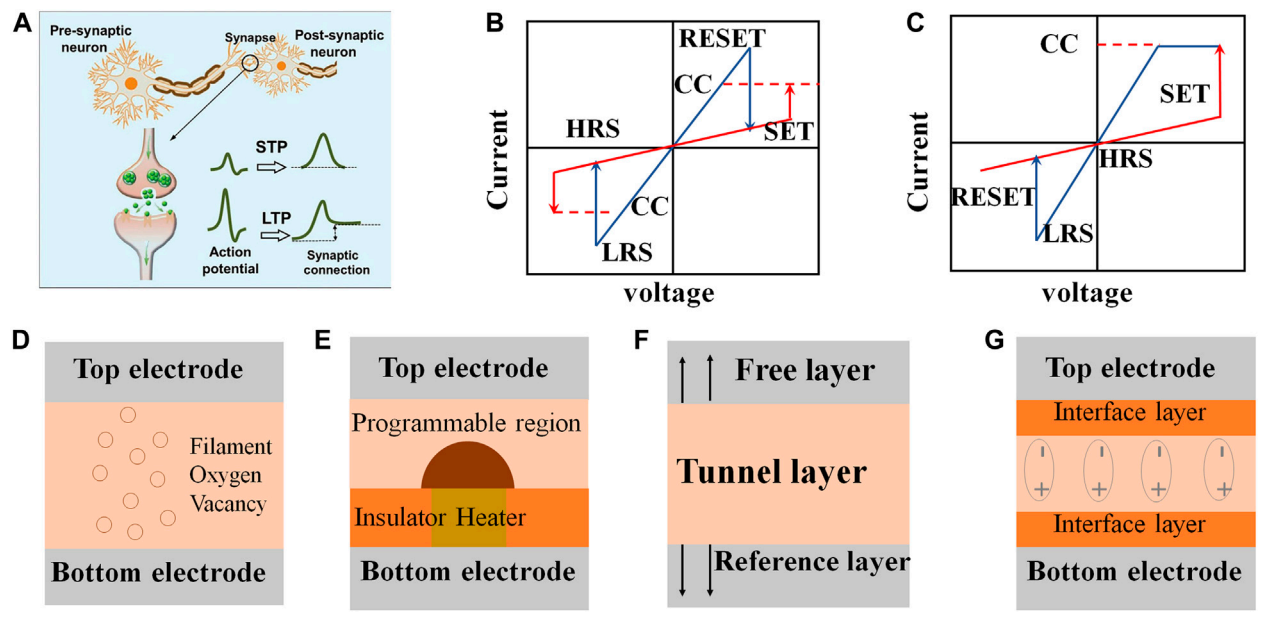

FIGURE 2 | (A) Schematic diagram of neurons and synapses [adapted from Hu et al. (2017)]. **(B)** Unipolar resistive switching mode. **(C)** Bipolar resistive switching mode. Device structure and working principle of **(D)** metallic filament device, **(E)** phase change device, **(F)** magnetic memristive device, and **(G)** ferroelectric memristive device.

circuit element after resistance, capacitance, and inductance. Its conductance can be changed by controlling the change of the voltage or current, similar to changes in synaptic weights. It can be used to simulate STP, LTP, STDP and SRDP, and is widely used in artificial neural networks (Kim et al., 2015; Tan et al., 2016; Hu et al., 2017; Wang H. et al., 2018; Choi et al., 2018b; Kim and Lee, 2018; Zhang S.-R. et al., 2019; Chen et al., 2019; Mikheev et al., 2019; Liang et al., 2020; Pereira et al., 2020; Wright et al., 2022). Its size can be reduced to less than 2 nm, the switching speed can be controlled within 1 ns, and it has lower operating power consumption (Wang M. et al., 2018; Xia and Yang, 2019; Marković et al., 2020). Besides, there is a wide range of materials available for the construction of memristors, which allows for the simulation of synaptic performance for various needs and the construction of crossbar array and artificial neuromorphic systems. The intermediate layer and electrode materials are crucial in the selection of memristors. In recent years, an increasing number of new materials have been discovered to be suitable for memristors, primarily electrode materials with varying activities (Cu, Ag, Ru, Pt, Pd, etc.) (Nayak et al., 2012; Tsuruoka et al., 2012; Chen et al., 2016; Zhang et al., 2017; Jang et al., 2019; Li et al., 2020), organic materials (egg protein, TTP, PMMA, PVA, etc.) (Liu et al., 2016), oxide materials (HfO_x, TaO_x, TiO_x and some multi-component oxides, etc.) (Choi et al., 2018a), sulfide materials (MoS_2, Cu_2S, and so on). More new materials have recently been demonstrated to be applicable to memristors (Ohno et al., 2011; Kuzum et al., 2012a; Yang et al., 2013; Tuma et al., 2016; Kim et al., 2017; Stoliar et al., 2017; Choi et al., 2018a; Wang Z. et al., 2018; Chen et al., 2021). At present, memristive-related devices can be roughly divided into metallic filament device, phase change device, magnetic memristive device, ferroelectric memristive device, the structure and operation mechanisms of them will be introduced in detail.

Metallic Filament Synapse

The structure of metallic filament synapse is typically "sandwich." This structure, as shown in **Figure 2D**, consists of a top electrode, a bottom electrode, and a middle resistive insulator layer. They are classified as abrupt memristors (only high- and low-resistance states) or gradient memristors (there are multiple resistance states, and even the resistance can change continuously). There are numerous theories about the resistive switching mechanism, with the metal conductive filament mechanism, the vacancy mechanism of other materials, or electrochemical metallization mechanism being the most widely accepted (Sawa, 2008; Waser, 2009; Wong et al., 2012).The electrode material of a resistive memristor is typically made of an active metal, such as silver or copper. When the top electrode metal loses electrons and becomes ionic, the bottom electrode gains electrons, and the intermediate dielectric layer forms a soft dielectric breakdown. Conductive filaments and synapses are converted from a low- to a high-resistance state. This is the SET process. When a reverse voltage is applied, the conductive filaments are disconnected, and the synapses transitions from a high-resistance to a low-resistance state, which is a RESET process. It is similar to the traditional electrochemical redox reaction. The resistance change in non-conductive filament resistive device is caused by defect migration under the action of the electric field, which causes the Schottky barrier or tunneling barrier to change uniformly in the device interface. There are two types of resistive switching modes in metallic filament synapse: single and bipolar (Choi et al., 2016), as shown in **Figures 2B–C**). The resistive switching phenomenon occurs under voltages of different polarities in the bipolar resistive switching mode, i.e., SET/RESET occurs under opposite voltage polarities. The resistive switching phenomenon has nothing to do with voltage polarity in the unipolar resistive switching mode, but only with voltage amplitude. Metallic filament synapses have a straightforward device structure, good scalability, superior complementary metal oxide semiconductor (CMOS) compatibility and low power consumption. Recent research on metallic filament synapses has received countless attention due to the potential in large-scale integration. Hu et al. proposed a Cu/ZnS/Pt device with an ultra-low set voltage of several millivolts (Hu et al., 2017). In this device, filament rupture and filament rejuvenation is restricted to a nanometer thick two layer interface region due to differing ion transport rates in the unoxidized and lightly oxidized layers. The device accurately simulates synaptic plasticity, as shown in **Figure 3A**, by employing repeated voltage pulses to achieve STP. In addition, as shown in **Figure 3B**, the PPF was observed, when the pulse interval time is reduced, the PPF index decreases, which is very similar to the situation in biological synapses. STP transitions to LTP as the pulse amplitude increases, as shown in **Figure 3C**, the process that may be related to the migration and diffusion of copper ions. Based on the device's STP and LTP behavior, it can be used to simulate the memory and forgetting processes of images.

Phase Change Synapse

Phase change synapses, like metallic filament synapse, typically have a sandwich structure with a top electrode, a bottom electrode, and a phase change material layer, as shown in **Figure 2E**. Sulfur-containing compounds, such as $Ge_2Sb_2Te_5$ (Wong et al., 2010; Zhang W. et al., 2019), are commonly used phase change materials. In most cases, a phase change mechanism means that the materials will change phase under certain conditions, and the device's conductance will differ before and after the phase change. There are numerous factors that influence phase transitions, including electro-induced phase transition (Driscoll et al., 2009) and thermally induced phase transition (Yang et al., 2019). During the SET process, a small amplitude voltage pulse is applied across the phase change synapse, which can cause the phase change material to crystallize and transform into a polycrystalline state, resulting in a low resistance value. The application of a relatively large voltage pulse during the RESET process causes the phase change material to locally melt and transform into an amorphous state, and its resistance value is high at this time. Multi-level resistance states of the phase change synapse can be achieved by modulating the relative ratio of the polycrystalline and amorphous states of the phase change material with voltage pulses and temperature. Its advantages include high scalability, fast operation speed, and low volatility (Lankhorst et al., 2005; Wang Q. et al., 2021). Kuzum et al. first used GST to fabricate a single phase change synaptic device (Kuzum et al., 2012a), they

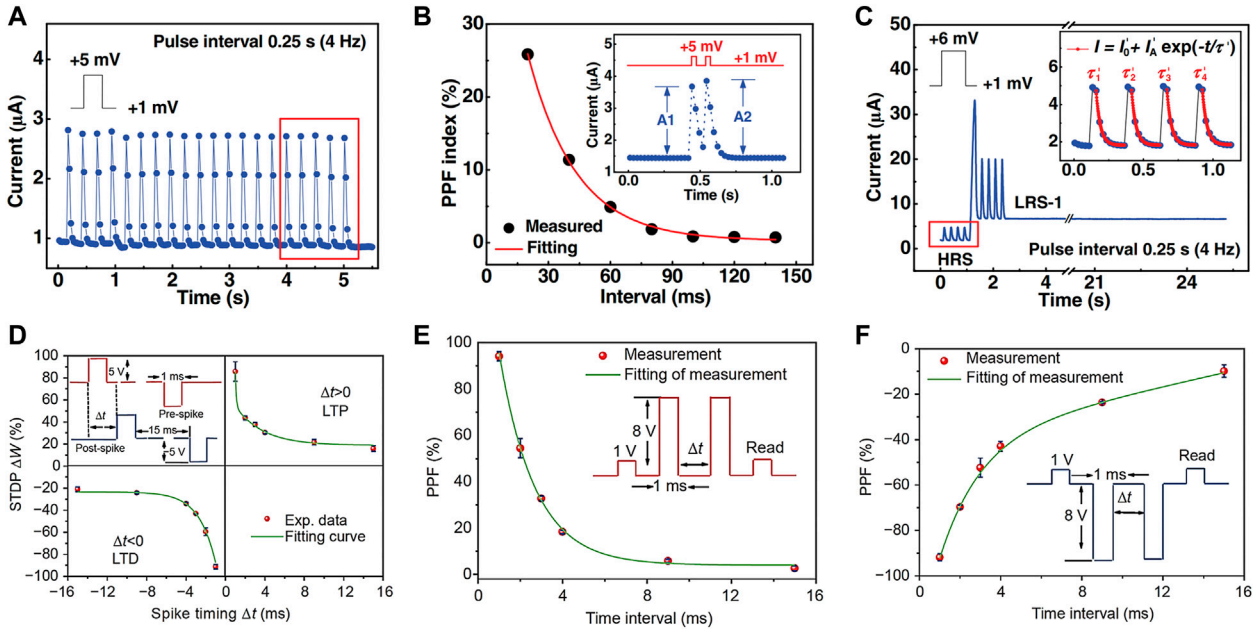

FIGURE 3 | (A) Applying voltage pulses with an amplitude of 5 Mv to achieve STP. **(B)** Simulation of the PPF and the change of the PPF index with the pulse interval. **(C)** Applying voltage pulses with an amplitude of 6 Mv to achieve LTP [adapted from Hu et al. (2017)]. **(D)** STDP characteristics of the ferroelectric memristors. **(E,F)** Characteristic curves of PPF [adapted from Yu et al. (2020)].

used voltage pulses of gradually increasing amplitude to accomplish conductivity modulation in 100 steps, while maintaining a good dynamic range. Wan et al. created nanoclusters of phase transition using a memristive structure (Wan et al., 2022). Under external stimulation, in the two AlNO dielectric layers, phase change nanoclusters were formed adaptively with distinct distribution patterns. After critical stimulation, the system may respond to stimulation strength and fire AP. Despite phase change synapse's conductance state can be modified by changing the programming conditions, phase change materials' crystallization and quenching processes are uncontrolled and unpredictable, resulting in nonlinear conductance changes that are incompatible with neural network learning.

Magnetic Memristive Synapse

Figure 2F depicts the magnetic memristive synapse's structure. Its basic structure is made up of three layers: the free layer, the tunnel layer, and the reference layer. When the number of electrons in the material's up and down spin directions is equal, the material as a whole has no magnetism. The material will exhibit magnetic properties when the number of electrons spinning up and down is unequal. In the magnetic memristive synapse, the reference layer's magnetization direction remains constant, while the magnetization direction of the free layer can be programmed to change, and the intermediate layer is referred to as the tunnel layer. The resistance of the magnetic memristive synapse is determined by the relative magnetization directions of the reference layer and the free layer. When the magnetization directions of the reference layer and the free layer are the same (P state), the resistance value of the magnetic memristive synapse is the lowest; when the magnetization directions are inconsistent (AP state), the resistance value of the magnetic memristive synapse is the highest. By directly passing a current through the magnetic memristive synapse, the free layer's electron spin direction can be modified, thereby changing the resistance state of the device. Luo's proposed a VCSK device with a FE/HM/MTJ structure (Luo et al., 2019). According to physical simulations, the resistance values can be modulated efficiently using voltage and STT's assistance.

Ferroelectric Memristive Synapse

The ferroelectric memristive synapse is a relatively new type of memristive synapse that has emerged in recent years, **Figure 2G** depicts its structure. It consists of a ferroelectric material layer and two electrode layers (Scott and Paz de Araujo, 1989). The resistance of the device can be gradually adjusted by inverting the ferroelectric domain by regulating the ferroelectric polarization (Garcia and Bibes, 2014; Guo R. et al., 2020). Multiple resistance states with bidirectional continuous reversibility can be acquired at the same time, similar to the change of synaptic weights. The ferroelectric memristive synapse has the advantages of fast read and write speed, low driving voltage, and high storage density, and it can overcome the shortcomings of the traditional resistive memristor's conductive filament instability and fracture, it has demonstrated outstanding characteristics such as high ON/OFF current ratios, high data storage density, fast switching speeds, and ultra-low power (Zucker and Regehr, 2002; Kullmann and Lamsa, 2007; Luo et al., 2022). Sayani Majumdar et al. proposed a ferroelectric tunnel junction based on a spin-coated 3 nm thick

ferroelectric poly (vinylidene fluoride-trifluoroethylene) [P(VDF-TrFE)] and realized the simulation of synaptic function (Majumdar et al., 2019), exhibiting analog switching behavior in the range of five orders of magnitude, reproducibly simulate LTP/STP, LTD/STD and STDP, in addition, the device has good stability and a large range of conductance variation. Yu et al. proposed an Au/$Hf_{0.5}Zr_{0.5}O_2/p^+$ -Si memristor structure (Yu et al., 2020). According to STDP learning rules, the stimulation sequence of the presynaptic membrane and the stimulation sequence of the postsynaptic membrane differs, resulting in an increase and decrease of synaptic connection between two neurons. STDP simulation is depicted in **Figure 3D**, by varying the pulse interval applied to the device, the change in synaptic weight can be successfully simulated. Furthermore, the device can simulate PPF. As shown in **Figure 3**(E-F), when the time interval between two pulses is long, the device's conductivity is low, and when the pulse interval is short, the conductivity is high, simulating the process of biological learning and forgetting.

ARTIFICIAL NEURAL NETWORKS

Neural networks are currently classified into many species. The most fundamental neural network structures are single layer perceptron (SLP) and multilayer perceptron (MLP). Convolutional neural network (CNN) is a feedforward neural network made up of artificial neurons and synapses that can respond to other units. CNN has a higher generalization ability than the MLP and has been used more widely. Spiking neural network (SNN) is a type of neural network developed in the field of neuroscience, it encodes information as time and frequency of pulses. It is commonly used to create neural system simulations that are similar to brains. The advent of memristors opens up a new avenue for the development of artificial neural networks. The synaptic properties and advantages of memristors allow the artificial neural network to perform more diverse functions in addition to learning and memory. Next, we will focus on the advances of the above artificial neural networks based on memristors.

Single Layer Perceptron and Multilayer Perceptron

The SLP contains an input layer and an output layer, and they are directly connected. The most common MLP also includes a hidden layer, all neurons in the previous layer are connected to all of the next layer's neurons. The structure of MLP is basically similar to a cascade perceptron, in which each lattice processing unit has a relatively complex output function, thus enhancing the performance of the network. Prezioso et al. constructed a cossbar structure network using a 12*12 memristor array (Prezioso et al., 2015). In this network, the simplest recognition of the letters Z, V, and N was achieved, and the tolerance of the network was proved by adding an error input picture of pixel gray value inversion to three letters. This structure allows running a single layer perceptron network, **Figure 4A** shows the single layer perceptron for classification of 3 × 3 binary images. Burr et al. realized a 3-layer perceptron based on $Pr_{1-x}Ca_xMnO_3$ (PCMO) PCM device (Burr et al., 2015). This perceptron contains 164,885 synapses and is able to learn handwritten digit classification from the MNIST dataset with 82.2% accuracy. Yao et al. used 1T1R device units to simulate synaptic properties (Yao et al., 2017), realized bidirectional device conductance modulation, and realized a 3-layer fully connected multilayer perceptron through a 128*8 1T1R memristor array. **Figure 4B** is the structure of a 1T1R array, in a row, cells are organized by connecting the transistor sources and the source line (SL) as well as connecting the transistor gates and the same word line (WL), whereas cells are organized by connecting the resistive memory's top electrode to the bit line (BL) in a column. The functional material of the memristor in the array is TaO/$HfAl_yO_x$, the device can achieve good gradation during both SET and RESET processes. **Figure 4B** also depicts the network's mapping to the 1T1R structure. **Figure 5** is a flow chart of the perceptron model. This model has been trained to tell the difference between one person's face and the faces of others. There are two steps to the process: training process and testing process. The training process consists of two sub-processes: inference and weight update. During training, conductance values are normalized to integers between 0 and 255. Therefore, the Yale database's gray-scale face image identification has been realized, and the 9,000 images' recognition rate with noise effect can reach 88.08%. Compared with the conventional neural network computing, the neural network based on 1T1R array has 1,000 times lower energy consumption in on-chip computing and 20 times lower energy consumption in off-chip computing, achieving a significant energy saving effect. Bayat et al. designed and fabricated a 20 × 20 cross-array (Bayat et al., 2018). In terms of devices, the intermediate functional layer of the memristor uses TiO_{2-x} and Al_2O_3 stacks, and the Al_2O_3 stack as the barrier layer makes the basic I-V characteristics of the device more nonlinear, and this nonlinear helps to suppress the leakage current problem in the 0T1R array of memristors. At the same time, the bottom electrode is deposited into a triangular shape during the fabrication of the device, this design can allow the functional layer to better cover the bottom electrode and it can also reduce the contact resistance of the top electrode. On the basis of this research result, the team further interconnected the memristor crossbar array with traditional CMOS peripheral circuits, and designed and implemented a single-hidden-layer multilayer perceptron for classification functions, increasing the hardware design complexity by more than 10 times, the classification accuracy of offline learning is as high as 97% or more.

Convolutional Neural Network

The CNN's essential components are the input layer, convolution layer, activation layer, pooling layer, fully connected layer, and output layer. Local connection and parameter sharing are two properties of CNNs. Each output is connected to all inputs by weights in a local connection. Each output neuron in a convolutional layer is fully connected in the channel direction but only has a few input neurons in the spatial direction. The use of the same parameters in numerous functions of a model is

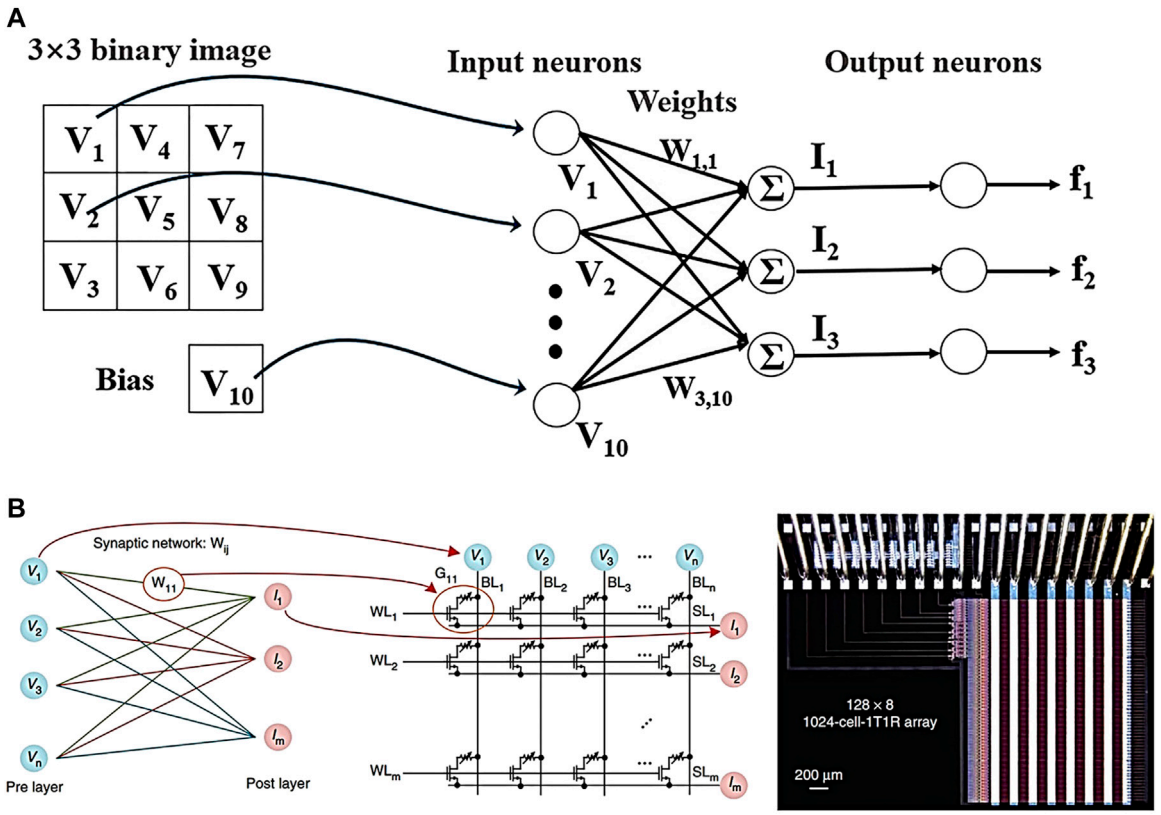

FIGURE 4 | (A) The single-layer perceptron for classification of 3 × 3 binary images [adapted from Prezioso et al. (2015)]. **(B)** The 1T1R architecture and the 1024-cell-1T1R array [adapted from Yao et al. (2017)].

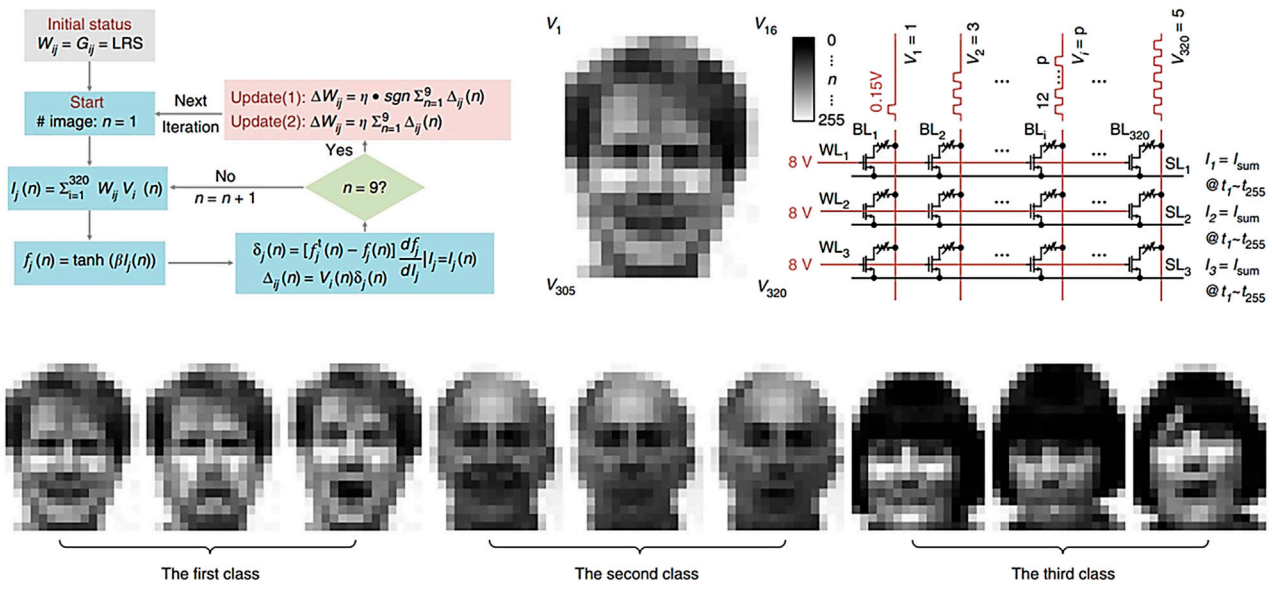

FIGURE 5 | Flowchart of the perceptron model [adapted from Yao et al. (2017)].

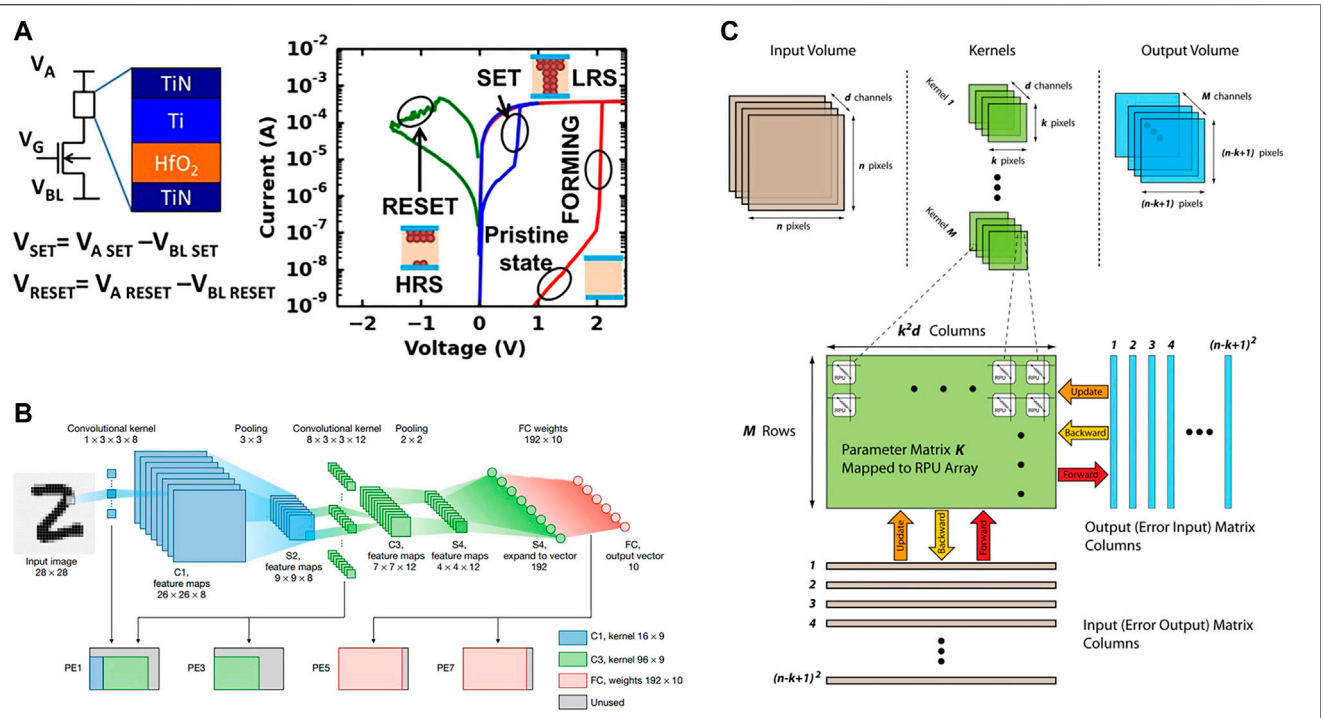

FIGURE 6 | (A) 1T-1R OxRAM device schematic and typical current–voltage OxRAM characteristics [adapted from Garbin et al. (2015)]. **(B)** Schematics of a convolutional layer showing the input volume, kernels, and the output volume [adapted from Gokmen et al. (2017)]. **(C)** Structure of the five-layer mCNN used for MNIST image recognition [adapted from Yao et al. (2020)].

referred to as parameter sharing. As a result, the convolutional neural network is more extensively utilized than the multi-layer perceptron and has a higher generalization capacity. Garbin et al. first used multiple HfO_2 based memristors to simulate some synaptic functions and realized the construction of CNN (Garbin et al., 2015). **Figure 6A** shows the structural schematic diagram and typical current-voltage characteristics of the 1T1R device. Based on experimental and theoretical research into the effects of device conditions, it has been discovered that recognition of high-fidelity visual patterns can be achieved even with large device variations, and the pattern recognition rate >94%. Gokmen et al. proposed a method of mapping convolution layer to memristor array by using the parallelism of hardware (Gokmen et al., 2017), and investigated how to train CNNs using memristors in detail, as illustrated in **Figure 6B**, proposing techniques for boundary and noise management to address the problem that noise and boundary constraints imposed by computations performed on the array affect the training accuracy of CNNs, and discuss the effects of random device variability on the network and how to resolve it, further exploring memristor-based Convolutional Neural Network Feasibility. Yao et al. successfully developed a multi-array memristor-based memory-computing integrated system (Yao et al., 2020), which is two orders of magnitude more energy efficient than the cutting-edge graphics processing unit (GPU) when processing convolutional neural networks (CNNs). **Figure 6C** shows the memristor-based hardware system. The network integrates a total of 8 memristor-based processing units, each PE unit contains a memristor array of 2048 units. Each memristor is connected to the transistor using the drain terminal, that is, a 1T1R structure. Each memristor array has 128 × 16 1T1R cells. The array has a highly repeatable multi-level conductivity state, which successfully proves the feasibility of full hardware implementation of the memory-computing integrated architecture. The researchers also constructed a five-layer convolutional neural network based on the above research. The array chip replaces the transistors at the bottom of classical computers with memristors, which greatly improves the computing power of computing devices with smaller power consumption and lower hardware costs, breaking through the limitations of the Von Neumann bottleneck of traditional computing frameworks to a certain extent. While greatly improving computing power, it achieves smaller power consumption and lower hardware cost.

Spiking Neural Network

In SNNs, the neuron model is accomplished through mathematical modeling of biological neurons or by describing the dynamics of neurons. SNNs are thought to offer more potential in terms of integration and energy consumption than ANNs due to the use of pulsed signals as the information transmission medium. Oh et al. explored the law of phase-change memristor resistance drift and resistance drift characteristics and applied it to the spiking neural network to

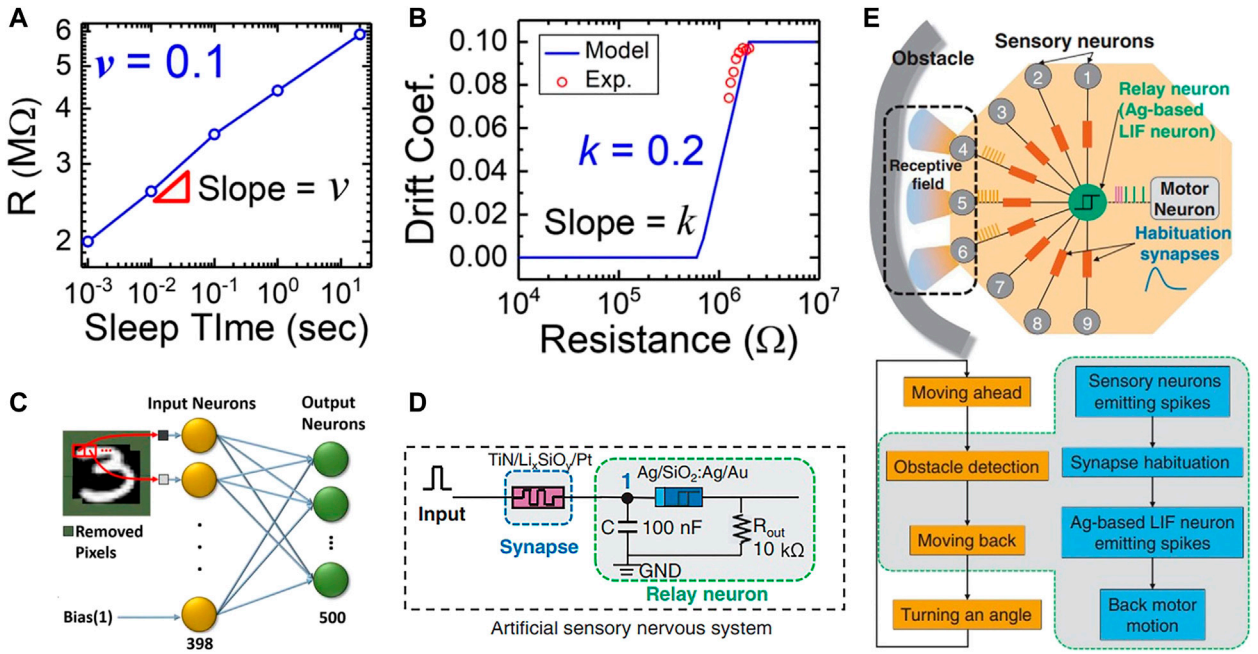

FIGURE 7 | (A) Resistance drift characteristics of GST PCM. **(B)** The drift coefficients for different initial resistances. **(C)** NN architecture with 398 input neurons and 500 output neurons with fully connected structure [adapted from Oh et al. (2018)]. **(D)** Memristor based artificial SNS circuit. **(E)** Schematic diagram of HSNN and flow chart of robot obstacle avoidance based on habitual learning rules [adapted from Wu Q. et al. (2020)].

recognize and classify MNIST handwritten digits (Oh et al., 2018), which improved the recognition accuracy. This property of variable memristors turns waste into treasure. **Figures 7A–B** briefly shows the resistance of the PCM drifts and the drift coefficients for different initial resistances. The initial resistance of the device is 2 megohms. As time goes by, the resistance of the device becomes larger. The curve's slope is 0.1, which represents the drift coefficient. **Figure 7C** depicts the designed spiking neural network structure diagram, mapping the synaptic weights to memristors' conductance values and online training after linear transformation, the results show that the SNN's accuracy can achieve 94.05% and 92.02% with 64-bit and 8-bit precision weights respectively, demonstrating that PCM resistance drift can be used to improve classification accuracy. Wang et al. proposed a brain-like computing method using memristors (Wang W. et al., 2018), they use the 1T1R structure combined with a spiking neural network for learning and recognition, the time difference between the spikes of different neurons constitutes the spatiotemporal encoding. Spatiotemporal patterns are learned via STDP, which are then recognized by appropriately potentiated/inhibited synapses. Wu et al. proposed an implementation scheme of constructing an artificial sensory neural system with habituation characteristics based on memristors (Wu Z. et al., 2020), and used habituation as a biological learning rule to construct a habit-spiking neural network that can be applied to autonomous cruise and obstacle avoidance of robots. First, the research team constructed sensory neurons based on memristors (TiN/Li_xSiO_y/Pt) and sensors. The neuron can sense external analog signals and convert them into real-time dynamic pulse signals, so as to realize the basic function of sensing and transmitting external signals. Subsequently, sensory neurons are further connected with relay neurons through synaptic devices (TiN/Li_xSiO_y/Pt), as shown in **Figure 7D**, to construct a habit perception system. The results show that the synaptic device has a habituation evolution trend of weights under continuous stimulation, which in turn affects the transmission efficiency of sensory neuron signals to relay neurons, so that the output of relay neurons presents a characteristic of decreasing frequency (i.e., habituation). Based on this habit feature, a habit spiking neural network is further constructed to realize the obstacle avoidance function of the robot. **Figure 7E** depicts the HSNN architecture for artificial intelligence navigation. It receives input from 9 sensory neurons, and 1 relay neuron is linked to sensory neurons *via* habitual synapses to process and deliver information. The results show that the artificial sensory nervous system based on memristor can effectively improve the robot's obstacle avoidance efficiency based on the habit learning rules. In addition, Boyn et al. demonstrate that ferroelectric nanosynaptic arrays can autonomously learn to recognize patterns in a predictable manner (Boyn et al., 2017b), demonstrating that organic FTJ memristors are feasible for spiking neural networks. Using memristor cross-arrays with symmetry and asymmetry, Kuzum et al. successfully implemented two main hippocampal learning mechanisms (Kuzum et al., 2012b), associative learning and sequential learning, in the presence of 30% noise in the input data. Associative learning successfully recalls 85% of the original patterns.

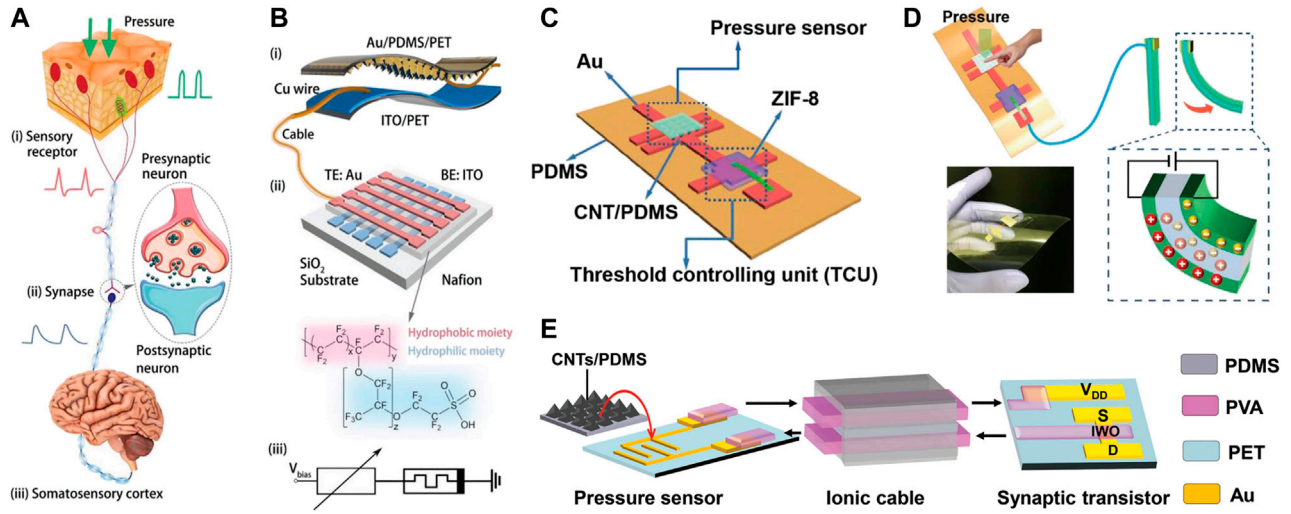

FIGURE 8 | (A) Illustration of the biological haptic perception system: **(i)** the sensory receptor, **(ii)** the synapse and **(iii)** the brain. **(B)** The artifical haptic perception system [adapted from Zhang C. et al. (2019)]. **(C)** Illustration of the complete artificial somatic reflex arc consisting of a pressure sensor, a TCU, and an electrochemical actuator. **(D)** Illustration of the complete artificial somatic reflex arc consisting of a pressure sensor, a TCU, and an electrochemical actuator [adapted from He et al. (2020)]. **(E)** Diagram illustrating the details of the Neu Tap [adapted from Wan et al. (2018)].

SENSORY NERVOUS SYSTEM

The sensory nervous system (SNS) in animals is the basic information perception mechanism that creates the interaction between organisms and their surroundings. External information is first sensed by numerous sensors (touch, vision, smell, etc.), then transported to the brain and processed, and finally a response to the external information is made. The sensory system serves as a link between the physical environment and inner experiences, allowing people and animals to perceive the outside world. Building an effective intelligent information perception system based on the functional properties of the biological sensory nerve system will considerably increase the system's information processing capability. Traditional sensing systems make use of electronic devices to sense and process information. Recently, because of the fast process speed and low power consumption, using new synaptic devices, particularly two terminal memristive devices, to imitate human perception has piqued the interest of researchers and has been regarded as a promising solution to build efficient artificial system (Wang J. et al., 2021; Wang M. et al., 2021; Li et al., 2021; Liang et al., 2022). In this section, we will introduce some recent advances in the research of tactile, auditory, visual and olfactory artificial systems.

Tactile Perception System

The skin is the largest sense organ in the human body, covering the entire body, which is an important organ for human to produce tactile. Every area of the skin is densely packed with sensors that detect external stimuli and actively measure their intensity. External pressure stimuli can be received by the sensors, and the resulting response signals are transmitted to the brain via the nervous system. Tactile signals are stored by the nervous system and become tactile memories, which help us interact with our surroundings more effectively. As a result, providing this perceptual learning capability to robots and prosthetics may expand their cognitive and adaptive capabilities. To accomplish this, artificial sensory neurons with perceptual learning must be created. Tee et al. first modeled mechanoreceptors by combining pressure sensors and ring oscillators to convert mechanical signals into action potentials in the form of digital frequency outputs (Tee et al., 2015). Zang et al. connected the pressure sensor to a multi-gate transistor through a polyvinyl alcohol ion cable (Zang et al., 2017), realizing the identification of convex and planar patterns, and realizing the perceptual learning of electronic skin. Subsequently, memristor-based pressure sensing systems also slowly appeared. Zhang et al. integrated a pressure sensor and a Nafion-based memristor to design an artificial tactile neuron system (Zhang C. et al., 2019). As shown in **Figures 8A–B**, the system consists of pressure sensors, Nafion-based memristors and corresponding circuits, which can imitate synaptic behaviors such as PPF, PPD, and STDP. The supervised learning method implemented in character recognition can achieve an accuracy of 91.7%, and it has advantages including low energy consumption, durability, biocompatibility, high sensitivity, and feasibility of large-scale integration. He et al. proposed an artificial system consisting of a pressure sensor, a threshold control unit, and an electrochemical actuator (He et al., 2020). As shown in **Figure 8C**, the system can mimic the human tactile function. The pressure sensor detects the pressure signal and converts it to an electrical signal, then transmitted the signal to the threshold control unit, which causes the electrochemical actuator to be activated, and completes the movement. **Figure 8D** shows the different

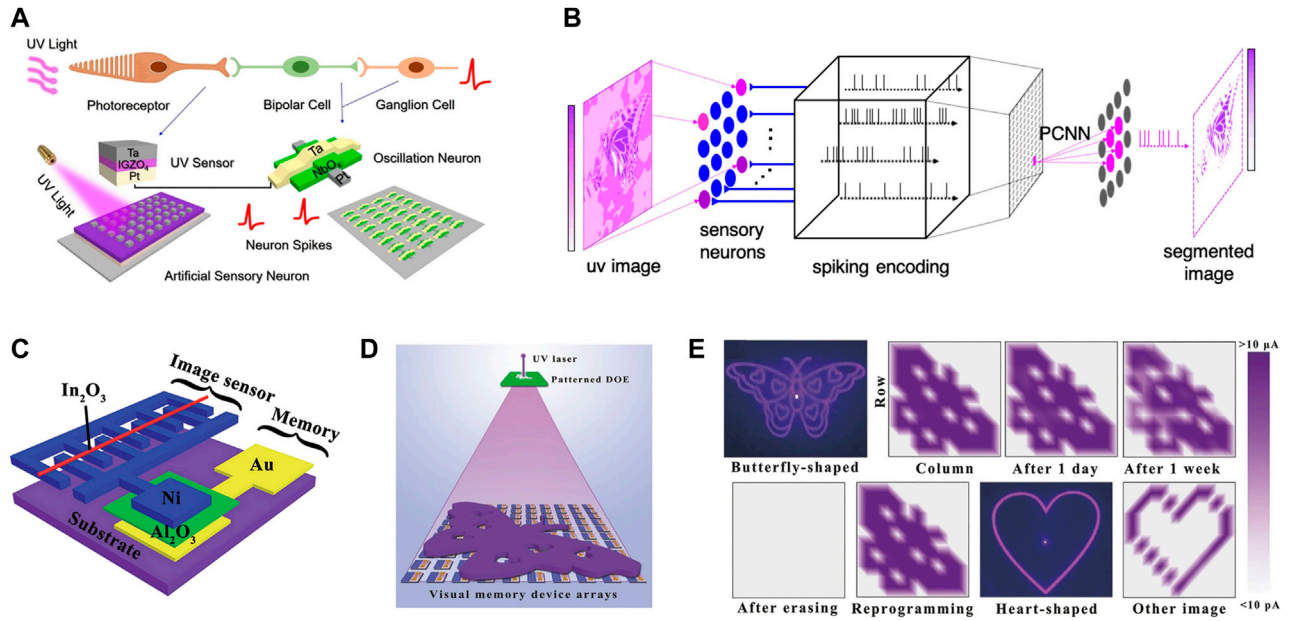

FIGURE 9 | (A) Schematic diagram showing the optical sensory neuron in the human vision system, schematic images of the artificial visual sensory neuron. **(B)** Schematic illustration of UV image segmentation in a pulse coupled neural network (PCNN) with UV artificial sensory neurons [adapted from Wu Z. et al. (2020)]. **(C)** Schematic diagram of artificial flexible visual memory system. **(D)** Schematic diagram to detect and memorize the information of light distribution which generated from a patterned DOE. **(E)** Information storage behaviors and effective reusability of the flexible visual memory device arrays for the applied patterned light [adapted from Chen et al. (2018)].

responses of the 3D printed manipulator prepared based on the principle of this system to soft and hard finger taps. For gentle taps, the fingers did not complete the gripping action. When tapped hard and the pressure levels above the threshold, the fingers bend and form a grasping position. Wan et al. proposed an artificial sensory neuron composed of resistive pressure sensors, ionic cables (Wan et al., 2018), and synaptic transistors. The structure is shown in **Figure 8E**. It can integrate and modulate the late spatiotemporal related tactile stimuli, and has a certain recognition ability. The recognition ability can be enhanced through repeated training, which is similar to the process of perceptual learning. Sun et al. proposed a self-powered artifical skin that incorporates RRAM and TENG (Sun et al., 2017). TENG converts mechanical touch signals into electrical signals, which are then store in RRAM, which can successfully memorize mechanical stimuli. Rahman et al. used a combination of stretchable pressure sensors (Rahman et al., 2020), phase-change oxide films, and STO memristor-based storage elements to realize fully functional Pacinian cells, thermoreceptors, and nociceptors. They are related to pressure, temperature, and pain, respectively, and will generate large responsive currents that can simulate real skin properties on artificial electronic skins, and even more complex functions such as threshold, relaxation, allodynia, and pain perception. allergies etc. Wang et al. proposed a memristive circuit based on a skin-like sensory processor (Wang et al., 2019). Its primary function is to process the external perceived feeling and convert it into the corresponding emotion. According to area overhead and power analysis, the proposed circuit has a simple structure and is simple to integrate.

Visual Perception System

The human visual perception system preprocesses the collected data before sending it to the cerebral cortex for deep recognition. The image information that has been processed is either short-term or long-term stored, depending on its importance. Traditional visual perception separates image perception, processing, and storage, resulting in redundant data that slows perception significantly. Inspired by the human visual system and the synaptic function of memristors, the researchers integrated optical perceptrons and memristors to provide new ideas for the fusion of optical learning, storage, computing and recognition. Wu et al. proposed an artificial sensory neuron that simultaneously senses and encodes optical information as electrical impulses (Wu Q. et al., 2020). **Figure 9A** shows a rough representation of the human visual system and the artificial visual sensory system magnetization direction. The researchers tested the device to show stable oscillatory behavior and UV sensing properties. The series combination of Pt/NbO_x/Ta oscillatory neurons and Ta/$IGZO_4$/Pt ultraviolet sensors constitutes artificial sensory neurons, which can be used to simulate the function of the human visual system. Similar to the biological visual system, an artificial sensory neuron can encode various UV inputs as spikes and display four different stable peak frequencies, this different oscillation frequency under different UV input signals, and then

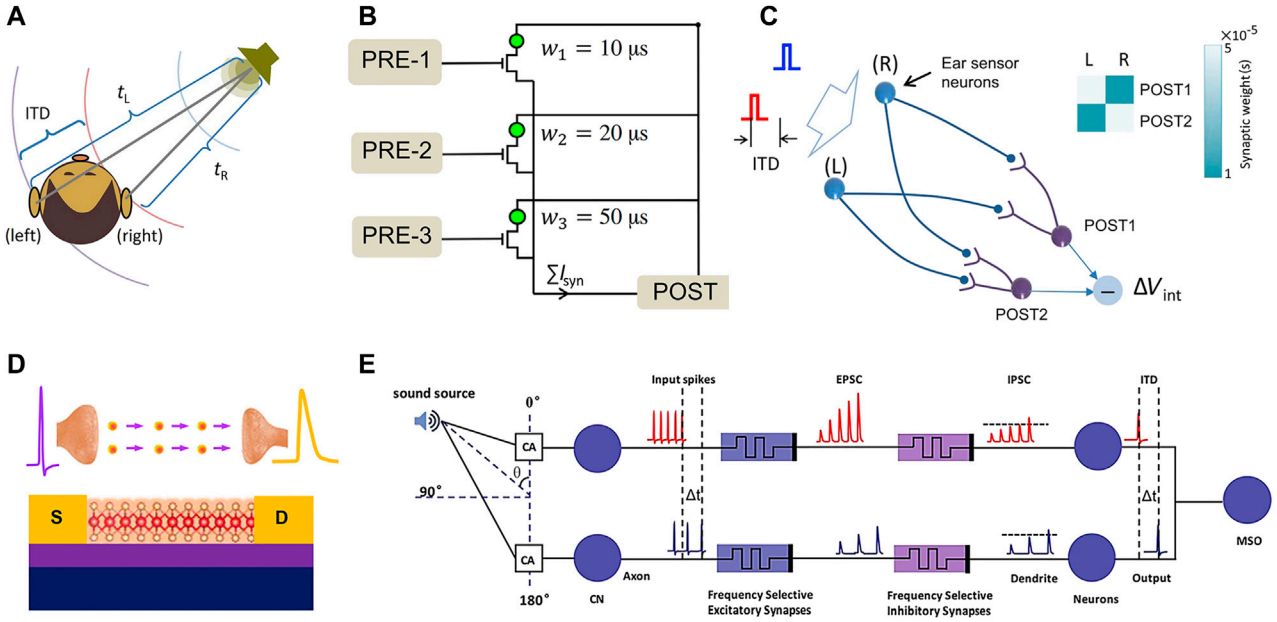

FIGURE 10 | (A) Schematic illustration of binaural effect, where the ITD provides an estimate of the direction of the sound. **(B)** Schematic SNN with three PREs and one POST. **(C)** Schematic structure of a 2 × 2 SNN to detect the sound direction from the ITD [adapted from Wang T. et al., 2021]. **(D)** Schematic diagrams of two-terminal devices based on monolayer MoS_2 with Joule heating. **(E)** Schematic picture of the working mechanism of synaptic computation for ITD-based sound localization [adapted from Sun et al. (2018)].

segmented by PCNN, as shown in **Figure 9B**, which means that the artificial sensory neuron can be used as an artificial vision system with output spikes, which can transfer information to a neuromorphic computing system for further information processing. The system is simple in structure and stable in performance, coupled with a CMOS-compatible manufacturing process, it is expected to become the development direction of neural robotic systems. Using UV-driven memristors, Chen. S et al. (Chen et al., 2018) built a basic framework to build an artificial flexible visual memory system, as illustrated in **Figure 9C**, **Figure 9D** depicts a typical memory array of 10 × 10 pixels used to demonstrate the imaging and memory of butterfly patterns. After a week of storage at room temperature, the visual memory array can retain the butterfly pattern in the mapping with almost no attenuation, as shown in **Figure 9E**. Wang et al. integrated photoelectric sensing, storage, and *in-situ* computing functions in a photomemristor array (Wang T.-Y. et al., 2021), it can greatly reduce the space occupied by multifunctional devices and improve the working efficiency of the chip. The neuromorphic computing power of the photonic memristor was validated with 86.7% accuracy using facial images of different people. Mu et al. connected discrete photodetectors in series with artificial neurons (Mu et al., 2021), increasing the complexity of signal recognition, transformation, and storage. IR-780 iodide, a small organic molecule, is used in memory devices as a charge trapping layer and a near infrared light-responsive film. Through optical and electrical modulation, artificial synaptic functions including STP, LTP and SRDP are achieved. In artificial sensory neuron systems, near-infrared light pulses can significantly increase the spike rate. Shan et al. proposed a novel plasmonic photomemristor that combines the LSPR effect with optical excitation, which can effectively improve the learning efficiency and accuracy of image recognition (Shan et al., 2022).

Auditory Perception System

The sensation created by sound waves acting on the auditory organs and processed by auditory centers at all levels is referred to as auditory. Interaural time difference (ITD) and interaural level difference (ILD) are the two main working mechanisms of the human brain for sound localization. When a sound source is closer to one ear than the other, there is a delay between the signal reaching the two ears. ILD is caused by the "shadow" effect, in which the listener's head is large in comparison to certain wavelengths of sound, acting as a barrier and casting shadows, the unique shape of the head, pinna, and torso can also act as a filter based on the location of the sound source (distance, azimuth, and elevation). Wang et al. presented a 1T1R-based SNN (Wang W. et al., 2018), two presynaptic neurons (representing the left and right ears, respectively) were used as input ports, and two postsynaptic neurons (representing the left and right ears, respectively) were developed to generate output internal voltage signals, as illustrated in **Figures 10A–C**. The position of the sound is estimated using ITD by measuring the internal potential difference of two postsynaptic neurons, accurately determining the location of the sound source. Sun et al. were the first to harness memristors' short-term plasticity to

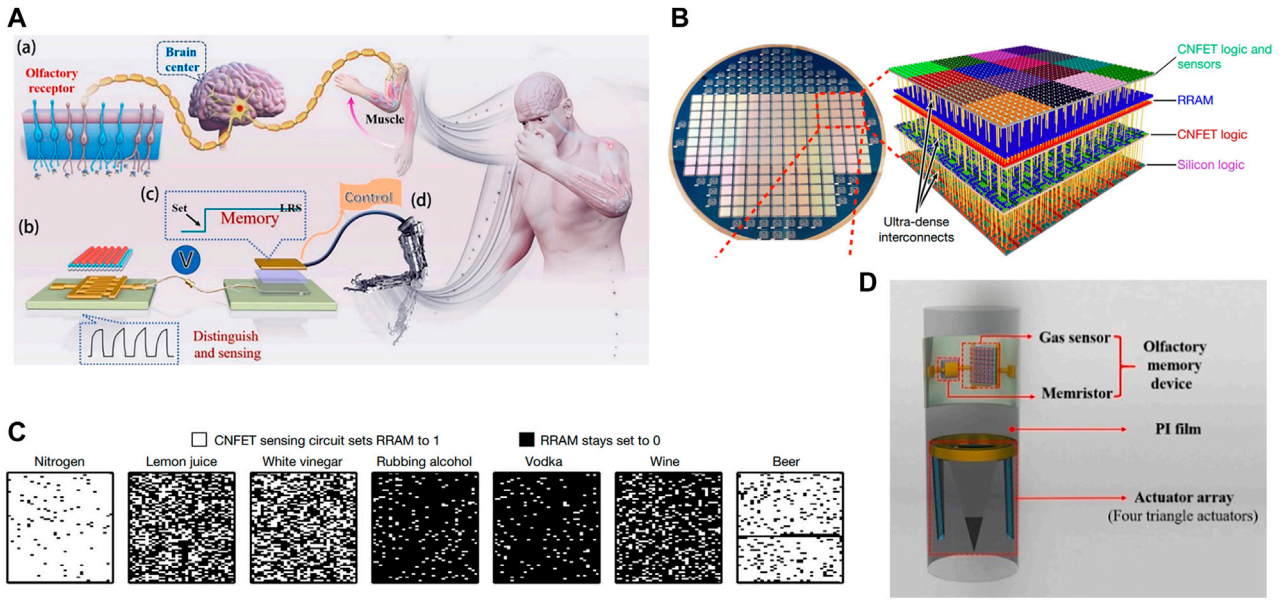

FIGURE 11 | (A) Overall comparison of the biological and artificial olfactory system [adapted from Gao et al. (2021)]. **(B)** Schematic diagram of a 3D nanosystem. **(C)** Test results for nanosystems [adapted from Shulaker et al. (2017)]. **(D)** Schematic illustration of bionic nose [adapted from Gao et al. (2021)].

enable precise temporal computation and to use the suppression of sound intensity and frequency-dependent synaptic connections for low-power temporal difference detection (Sun et al., 2018). The device diagram and working mechanism of ITD-based sound synaptic computing is shown in **Figures 10D–E**.

Olfactory Perception System

The biological olfactory perception system has important implications for organisms in food intake, emotional response, species identification, and predation or avoidance. Researchers have created artificial olfactory systems based on the olfactory system (Wang T. et al., 2021). **Figure 11A** depicts a detailed comparison of biological and synthetic olfactory systems. The olfactory system of humans is divided into three parts: olfactory receptors, brain centers, and muscles. Olfactory receptors respond to specific gas molecules by generating electrochemical potentials that are transmitted to the brain center via olfactory nerve fibers. Brain centers memorize smells and give specific smell-related instructions, such as controlling muscle contractions and raising arms. Shulaker et al. developed a system for sensing and classifying ambient gases that uses resistive memristors and carbon nanotube field effect transistors (Shulaker et al., 2017). The 3D nanosystem is depicted schematically in **Figure 11B**, it is made up of four integrated vertical layers linked by vertical interconnects: CNFET logic and sensors, RRAM, CNFET logic and silicon FET logic. The system classifies seven common gases, such as lemon juice and steam from white vinegar, as shown in **Figure 11C**, it identifies gases by comparing raw sensor data with previously learned expected responses. Gao et al. proposed a synthetic odor using Sr-ZnO based gas sensors (Gao et al., 2021), HfO_x based memristors, and electrochemical actuators. In addition to gas identification, the Sr-ZnO gas sensor can take some measures to protect the system from toxic gases. For example, the Sr-ZnO gas sensor can sense and identify NH_3 through resistance change and transmit the signal to the memristor, information is preserved by changing the resistance state of the memristor. Simultaneously, the action potential is transmitted to the arm's skeletal muscle fibers, which eventually move the hand to cover the hand, similar to the self-protection effect of covering one's hand with one's hand when inhaling noxious NH_3. **Figure 11D** depicts a schematic diagram of the fabricated bionic nose. Furthermore, Iwata proposed using metal oxide-based memristors as gas sensor outputs to differentiate different gaseous acetone and EtOH based on the extracted transient responses (Iwata et al., 2019). The device is simple and miniaturized, with the benefit of system miniaturization. Vidiš proposed a $Pt/TiO_2/Pt$ capacitor-like structure that can combine gas sensing and resistive switching capabilities to form a simple device (Vidiš et al., 2019). It functions as a gas-triggered switch and a gas sensor with memory. Wen proposed a new type of gas accumulation flow sensor based on memristor (Wen et al., 2019), which can measure the accumulated gas flow by combining the resistance of the memristor and the interception of the pipeline area, the measurement range is about 0–20 m^3, and the sensitivity in the effective range is about 28.44 Ω/m^3. To reduce measurement errors, Adeyemo proposed a TiO_2-based m (1 × n) for gas detection memristor arrays (Adeyemo et al., 2017). Khandelwal proposed a new memristor spice model that combines the development of a fault model capable of simulating gas sensing behavior with/without fault for simulation and integration with design automation tools (Khandelwal et al., 2019).

SUMMARY AND PERSPECTIVES

In this review, we primarily introduced new types of memristive-related devices, such as metallic filament synapse, phase change synapse, magnetic memristive synapse, ferroelectric memristive synapse. Simultaneously, we introduced the fundamental properties of memristive-related devices that are conducive to mimick the behavior of biological synapses and construct an artificial neural morphological system. Then, the application of memristors memristive-related devices in neuromorphic computing systems and perception were introduced. In conclusion, emerging neuromorphic computing and perception devices hold great promise as building blocks for next-generation computing and robotic systems. However, many issues remain to be resolved in the hardware implementation of neural networks. To begin with, the stability of the memristor is difficult to guarantee, which is one of the major issues impeding memristor research. The SET/RESET current fluctuates a lot, which affects the calculation results. As a result, improving the uniformity and reliability of device parameters will remain the primary research focus in the future. In addition, the synaptic properties of memristor devices still need to be improved. For example, the multivalued conductance tuning properties of memristors are currently studied only in terms of continuous changes in conductance under continuous pulse applications, whereas for practical applications, stable and nonvolatile individual conductance states are required. As a result, how to define the multi-value of memristor's changing conductivity from the standpoint of device engineering and how to improve the stable multi-value characteristics of memristor's synaptic device are major issues in the actual hardware implementation of memristor's synaptic device. According to the current research findings, memristor arrays outperform traditional CMOS logic circuits in parallel computing. However, memristor synaptic devices' analog computing characteristics are not fully compatible with peripheral CMOS digital circuits. Furthermore, the noble metal electrodes commonly used in memristors are incompatible with mature CMOS processes, which is a pressing issue that must be addressed. Furthermore, the majority of research on memristor-based sensing applications is based on simulating a specific sense and simple processing, such as touch, vision, smell, and so on, and the processing capacity is extremely limited. The external environment in which the human perceptual memory system is located is more complex. It can sense touch, pain, and temperature at the same time on a very small sensory unit, and it can sense external pressure and different temperatures at the same time and process information. As a result, developing a device system with multi-sensing and diverse functions to close the gap with application requirements, developing reliable three-dimensional integration technology and flexible memristive materials, new nanotechnology and multi-sensing devices will be the main focus in the future. Finally, the study of the brain, neural computing, and sensing systems is still in its initial stages. Making fundamental advances and fully exploiting the application potential of memristive devices in neural computing and sensing simulation need the joint efforts of various disciplines, including material science, biology, chemistry, electronics, computer science and so on.

AUTHOR CONTRIBUTIONS

QW and JW conceptualized the concept and wrote the manuscript. YZ, LZ and CC participated in writing the manuscript. All authors contributed to the article and approved the submitted version.

REFERENCES

Adeyemo, A., Jabir, A., Mathew, J., Martinelli, E., Di Natale, C., and Ottavi, M. (2017). "Reliable Gas Sensing with Memristive Array," in 2017 IEEE 23rd International Symposium on On-Line Testing and Robust System Design (IOLTS): IEEE), 244–246. doi:10.1109/iolts.2017.8046228

Backus, J. (1978). Can programming be liberated from the von Neumann style? *Commun. ACM* 21 (8), 613–641. doi:10.1145/359576.359579

Bayat, F. M., Prezioso, M., Chakrabarti, B., Nili, H., Kataeva, I., and Strukov, D. (2018). Implementation of Multilayer Perceptron Network with Highly Uniform Passive Memristive Crossbar Circuits. *Nat. Commun.* 9 (1), 2331. doi:10.1038/s41467-018-04482-4

Boyn, S., Grollier, J., Lecerf, G., Xu, B., Locatelli, N., Fusil, S., et al. (2017a). Learning through Ferroelectric Domain Dynamics in Solid-State Synapses. *Nat. Commun.* 8 (1), 14736–14737. doi:10.1038/ncomms14736

Boyn, S., Grollier, J., Lecerf, G., Xu, B., Locatelli, N., Fusil, S., et al. (2017b). Learning through Ferroelectric Domain Dynamics in Solid-State Synapses. *Nat. Commun.* 8, 14736. doi:10.1038/ncomms14736

Burr, G. W., Shelby, R. M., Sidler, S., di Nolfo, C., Jang, J., Boybat, I., et al. (2015). Experimental Demonstration and Tolerancing of a Large-Scale Neural Network (165 000 Synapses) Using Phase-Change Memory as the Synaptic Weight Element. *IEEE Trans. Electron Devices* 62 (11), 3498–3507. doi:10.1109/ted.2015.2439635

Caporale, N., and Dan, Y. (2008). Spike Timing-dependent Plasticity: a Hebbian Learning Rule. *Annu. Rev. Neurosci.* 31, 25–46. doi:10.1146/annurev.neuro.31.060407.125639

Chang, T., Jo, S.-H., Kim, K.-H., Sheridan, P., Gaba, S., and Lu, W. (2011). Synaptic Behaviors and Modeling of a Metal Oxide Memristive Device. *Appl. Phys. A* 102 (4), 857–863. doi:10.1007/s00339-011-6296-1

Chen, F., Zhou, Y., Zhu, Y., Zhu, R., Guan, P., Fan, J., et al. (2021). Recent Progress in Artificial Synaptic Devices: Materials, Processing and Applications. *J. Mat. Chem. C* 9 (27), 8372–8394. doi:10.1039/d1tc01211h

Chen, S., Lou, Z., Chen, D., and Shen, G. (2018). An Artificial Flexible Visual Memory System Based on an UV-Motivated Memristor. *Adv. Mat.* 30 (7), 1705400. doi:10.1002/adma.201705400

Chen, W., Fang, R., Balaban, M. B., Yu, W., Gonzalez-Velo, Y., Barnaby, H. J., et al. (2016). A CMOS-Compatible Electronic Synapse Device Based on Cu/SiO2/W Programmable Metallization Cells. *Nanotechnology* 27 (25), 255202. doi:10.1088/0957-4484/27/25/255202

Chen, Y., Qiu, W., Wang, X., Liu, W., Wang, J., Dai, G., et al. (2019). Solar-blind SnO2 Nanowire Photo-Synapses for Associative Learning and Coincidence Detection. *Nano Energy* 62, 393–400. doi:10.1016/j.nanoen.2019.05.064

Choi, B. J., Torrezan, A. C., Strachan, J. P., Kotula, P. G., Lohn, A. J., Marinella, M. J., et al. (2016). High-Speed and Low-Energy Nitride Memristors. *Adv. Funct. Mat.* 26 (29), 5290–5296. doi:10.1002/adfm.201600680

Choi, S., Jang, S., Moon, J.-H., Kim, J. C., Jeong, H. Y., Jang, P., et al. (2018a). A Self-Rectifying TaOy/nanoporous TaOx Memristor Synaptic Array for Learning

and Energy-Efficient Neuromorphic Systems. *NPG Asia Mater* 10 (12), 1097–1106. doi:10.1038/s41427-018-0101-y

Choi, S., Tan, S. H., Li, Z., Kim, Y., Choi, C., Chen, P.-Y., et al. (2018b). SiGe Epitaxial Memory for Neuromorphic Computing with Reproducible High Performance Based on Engineered Dislocations. *Nat. Mater* 17 (4), 335–340. doi:10.1038/s41563-017-0001-5

Chua, L. (1971). Memristor-the Missing Circuit Element. *IEEE Trans. Circuit Theory* 18 (5), 507–519. doi:10.1109/tct.1971.1083337

Collobert, R., and Weston, J. (2008). "A Unified Architecture for Natural Language Processing: Deep Neural Networks with Multitask Learning," in Proceedings of the 25th international conference on Machine learning, 160–167.

Cooper, L. N., and Bear, M. F. (2012). The BCM Theory of Synapse Modification at 30: Interaction of Theory with Experiment. *Nat. Rev. Neurosci.* 13 (11), 798–810. doi:10.1038/nrn3353

Driscoll, T., Kim, H.-T., Chae, B.-G., Di Ventra, M., and Basov, D. N. (2009). Phase-transition Driven Memristive System. *Appl. Phys. Lett.* 95 (4), 043503. doi:10.1063/1.3187531

Gao, Z., Chen, S., Li, R., Lou, Z., Han, W., Jiang, K., et al. (2021). An Artificial Olfactory System with Sensing, Memory and Self-Protection Capabilities. *Nano Energy* 86, 106078. doi:10.1016/j.nanoen.2021.106078

Garbin, D., Vianello, E., Bichler, O., Rafhay, Q., Gamrat, C., Ghibaudo, G., et al. (2015). HfO2-Based OxRAM Devices as Synapses for Convolutional Neural Networks. *IEEE Trans. Electron Devices* 62 (8), 2494–2501. doi:10.1109/ted.2015.2440102

Garcia, V., and Bibes, M. (2014). Ferroelectric Tunnel Junctions for Information Storage and Processing. *Nat. Commun.* 5, 4289. doi:10.1038/ncomms5289

Gokmen, T., Onen, M., and Haensch, W. (2017). Training Deep Convolutional Neural Networks with Resistive Cross-Point Devices. *Front. Neurosci.* 11, 538. doi:10.3389/fnins.2017.00538

Guo, L., Wang, T., Wu, Z., Wang, J., Wang, M., Cui, Z., et al. (2020a). Portable Food-Freshness Prediction Platform Based on Colorimetric Barcode Combinatorics and Deep Convolutional Neural Networks. *Adv. Mat.* 32 (45), 2004805. doi:10.1002/adma.202004805

Guo, R., Lin, W., Yan, X., Venkatesan, T., and Chen, J. (2020b). Ferroic Tunnel Junctions and Their Application in Neuromorphic Networks. *Appl. Phys. Rev.* 7 (1), 011304. doi:10.1063/1.5120565

Guo, R., Zhou, Y., Wu, L., Wang, Z., Lim, Z., Yan, X., et al. (2018). Control of Synaptic Plasticity Learning of Ferroelectric Tunnel Memristor by Nanoscale Interface Engineering. *ACS Appl. Mat. Interfaces* 10 (15), 12862–12869. doi:10.1021/acsami.8b01469

He, K., Liu, Y., Wang, M., Chen, G., Jiang, Y., Yu, J., et al. (2020). An Artificial Somatic Reflex Arc. *Adv. Mat.* 32 (4), 1905399. doi:10.1002/adma.201905399

He, Y., Yang, Y., Nie, S., Liu, R., and Wan, Q. (2018). Electric-double-layer Transistors for Synaptic Devices and Neuromorphic Systems. *J. Mat. Chem. C* 6 (20), 5336–5352. doi:10.1039/c8tc00530c

Hinton, G., Deng, L., Yu, D., Dahl, G., Mohamed, A.-r., Jaitly, N., et al. (2012). Deep Neural Networks for Acoustic Modeling in Speech Recognition: The Shared Views of Four Research Groups. *IEEE Signal Process. Mag.* 29 (6), 82–97. doi:10.1109/msp.2012.2205597

Hu, L., Fu, S., Chen, Y., Cao, H., Liang, L., Zhang, H., et al. (2017). Ultrasensitive Memristive Synapses Based on Lightly Oxidized Sulfide Films. *Adv. Mat.* 29 (24), 1606927. doi:10.1002/adma.201606927

Huang, H., Ge, C., Liu, Z., Zhong, H., Guo, E., He, M., et al. (2021). Electrolyte-gated Transistors for Neuromorphic Applications. *J. Semicond.* 42 (1), 013103. doi:10.1088/1674-4926/42/1/013103

Iwata, T., Ono, K., Yoshikawa, T., and Sawada, K. (2019). "Gas Discrimination Based on Single-Device Extraction of Transient Sensor Response by a MetalOxide Memristor toward Olfactory Sensor Array," in *2019 IEEE SENSORS: IEEE)*, 1–4.

Jang, B. C., Kim, S., Yang, S. Y., Park, J., Cha, J.-H., Oh, J., et al. (2019). Polymer Analog Memristive Synapse with Atomic-Scale Conductive Filament for Flexible Neuromorphic Computing System. *Nano Lett.* 19 (2), 839–849. doi:10.1021/acs.nanolett.8b04023

Khandelwal, S., Bala, A., Gupta, V., Ottavi, M., Martinelli, E., and Jabir, A. (2019). "Fault Modeling and Simulation of Memristor Based Gas Sensors," in 2019 IEEE 25th International Symposium on On-Line Testing and Robust System Design (IOLTS): IEEE), 58–59. doi:10.1109/iolts.2019.8854459

Kim, K., Chen, C.-L., Truong, Q., Shen, A. M., and Chen, Y. (2013). A Carbon Nanotube Synapse with Dynamic Logic and Learning. *Adv. Mat.* 25 (12), 1693–1698. doi:10.1002/adma.201203116

Kim, M.-K., and Lee, J.-S. (2018). Short-Term Plasticity and Long-Term Potentiation in Artificial Biosynapses with Diffusive Dynamics. *ACS Nano* 12 (2), 1680–1687. doi:10.1021/acsnano.7b08331

Kim, S., Du, C., Sheridan, P., Ma, W., Choi, S., and Lu, W. D. (2015). Experimental Demonstration of a Second-Order Memristor and its Ability to Biorealistically Implement Synaptic Plasticity. *Nano Lett.* 15 (3), 2203–2211. doi:10.1021/acs.nanolett.5b00697

Kim, S., Kim, H., Hwang, S., Kim, M.-H., Chang, Y.-F., and Park, B.-G. (2017). Analog Synaptic Behavior of a Silicon Nitride Memristor. *ACS Appl. Mat. Interfaces* 9 (46), 40420–40427. doi:10.1021/acsami.7b11191

Kullmann, D. M., and Lamsa, K. P. (2007). Long-term Synaptic Plasticity in Hippocampal Interneurons. *Nat. Rev. Neurosci.* 8 (9), 687–699. doi:10.1038/nrn2207

Kuzum, D., Jeyasingh, R. G. D., Lee, B., and Wong, H.-S. P. (2012a). Nanoelectronic Programmable Synapses Based on Phase Change Materials for Brain-Inspired Computing. *Nano Lett.* 12 (5), 2179–2186. doi:10.1021/nl201040y

Kuzum, D., Jeyasingh, R. G. D., Yu, S., and Wong, H.-S. P. (2012b). Low-Energy Robust Neuromorphic Computation Using Synaptic Devices. *IEEE Trans. Electron Devices* 59 (12), 3489–3494. doi:10.1109/ted.2012.2217146

Lankhorst, M. H. R., Ketelaars, B. W. S. M. M., and Wolters, R. A. M. (2005). Low-cost and Nanoscale Non-volatile Memory Concept for Future Silicon Chips. *Nat. Mater* 4 (4), 347–352. doi:10.1038/nmat1350

LeCun, Y., Bengio, Y., and Hinton, G. (2015). Deep Learning. *Nature* 521 (7553), 436–444. doi:10.1038/nature14539

Li, F., Wang, R., Song, C., Zhao, M., Ren, H., Wang, S., et al. (2021). A Skin-Inspired Artificial Mechanoreceptor for Tactile Enhancement and Integration. *ACS Nano* 15 (10), 16422–16431. doi:10.1021/acsnano.1c05836

Li, J., Yang, Y., Yin, M., Sun, X., Li, L., and Huang, R. (2020). Electrochemical and Thermodynamic Processes of Metal Nanoclusters Enabled Biorealistic Synapses and Leaky-Integrate-And-Fire Neurons. *Mat. Horiz.* 7 (1), 71–81. doi:10.1039/c9mh01206k

Liang, K., Wang, R., Huo, B., Ren, H., Li, D., Wang, Y., et al. (2022). Fully Printed Optoelectronic Synaptic Transistors Based on Quantum Dot-Metal Oxide Semiconductor Heterojunctions. *ACS Nano*. doi:10.1021/acsnano.2c00439

Liang, X., Li, Z., Liu, L., Chen, S., Wang, X., and Pei, Y. (2020). Artificial Synaptic Transistor with Solution Processed InOx Channel and AlOx Solid Electrolyte Gate. *Appl. Phys. Lett.* 116 (1), 012102. doi:10.1063/1.5120069

Liu, G., Wang, C., Zhang, W., Pan, L., Zhang, C., Yang, X., et al. (2016). Organic Biomimicking Memristor for Information Storage and Processing Applications. *Adv. Electron. Mat.* 2 (2), 1500298. doi:10.1002/aelm.201500298

Luo, S., Xu, N., Guo, Z., Zhang, Y., Hong, J., and You, L. (2019). Voltage-Controlled Skyrmion Memristor for Energy-Efficient Synapse Applications. *IEEE Electron Device Lett.* 40 (4), 635–638. doi:10.1109/led.2019.2898275

Luo, Z., Wang, Z., Guan, Z., Ma, C., Zhao, L., Liu, C., et al. (2022). High-precision and Linear Weight Updates by Subnanosecond Pulses in Ferroelectric Tunnel Junction for Neuro-Inspired Computing. *Nat. Commun.* 13 (1), 699. doi:10.1038/s41467-022-28303-x

Lynch, G. S., Gribkoff, V. K., and Deadwyler, S. A. (1976). Long Term Potentiation Is Accompanied by a Reduction in Dendritic Responsiveness to Glutamic Acid. *Nature* 263 (5573), 151–153. doi:10.1038/263151a0

Majumdar, S., Tan, H., Qin, Q. H., and van Dijken, S. (2019). Energy-Efficient Organic Ferroelectric Tunnel Junction Memristors for Neuromorphic Computing. *Adv. Electron. Mat.* 5 (3), 1800795. doi:10.1002/aelm.201800795

Malenka, R. C., Nicoll, R. A., and Qin, A, R. (1999). Long-term Potentiation-Aa Decade of Progress? *Science* 285 (5435), 1870–1874. doi:10.1126/science.285.5435.1870

Mao, H., He, Y., Chen, C., Zhu, L., Zhu, Y., Zhu, Y., et al. (2021). A Spiking Stochastic Neuron Based on Stacked InGaZnO Memristors. *Adv. Elect. Mater.* 8 (2), 2100918. doi:10.1002/aelm.202100918

Marković, D., Mizrahi, A., Querlioz, D., and Grollier, J. (2020). Physics for Neuromorphic Computing. *Nat. Rev. Phys.* 2 (9), 499–510.

Markram, H. (2006). The Blue Brain Project. *Nat. Rev. Neurosci.* 7 (2), 153–160. doi:10.1038/nrn1848

Mikheev, V., Chouprik, A., Lebedinskii, Y., Zarubin, S., Matveyev, Y., Kondratyuk, E., et al. (2019). Ferroelectric Second-Order Memristor. *ACS Appl. Mat. Interfaces* 11 (35), 32108–32114. doi:10.1021/acsami.9b08189

Mu, B., Guo, L., Liao, J., Xie, P., Ding, G., Lv, Z., et al. (2021). Near-Infrared Artificial Synapses for Artificial Sensory Neuron System. *Small* 17 (38), 2103837. doi:10.1002/smll.202103837

Nayak, A., Ohno, T., Tsuruoka, T., Terabe, K., Hasegawa, T., Gimzewski, J. K., et al. (2012). Controlling the Synaptic Plasticity of a Cu2S Gap-Type Atomic Switch. *Adv. Funct. Mat.* 22 (17), 3606–3613. doi:10.1002/adfm.201200640

Neves, G., Cooke, S. F., and Bliss, T. V. P. (2008). Synaptic Plasticity, Memory and the hippocampus: a Neural Network Approach to Causality. *Nat. Rev. Neurosci.* 9 (1), 65–75. doi:10.1038/nrn2303

Oh, S., Shi, Y., Liu, X., Song, J., and Kuzum, D. (2018). Drift-Enhanced Unsupervised Learning of Handwritten Digits in Spiking Neural Network with PCM Synapses. *IEEE Electron Device Lett.* 39 (11), 1768–1771. doi:10.1109/led.2018.2872434

Ohno, T., Hasegawa, T., Tsuruoka, T., Terabe, K., Gimzewski, J. K., and Aono, M. (2011). Short-term Plasticity and Long-Term Potentiation Mimicked in Single Inorganic Synapses. *Nat. Mater* 10 (8), 591–595. doi:10.1038/nmat3054

Pereira, M., Deuermeier, J., Nogueira, R., Carvalho, P. A., Martins, R., Fortunato, E., et al. (2020). Noble-Metal-Free Memristive Devices Based on IGZO for Neuromorphic Applications. *Adv. Electron. Mat.* 6 (10), 2000242. doi:10.1002/aelm.202000242

Pickett, M. D., and Stanley Williams, R. (2012). Sub-100 fJ and Sub-nanosecond Thermally Driven Threshold Switching in Niobium Oxide Crosspoint Nanodevices. *Nanotechnology* 23 (21), 215202. doi:10.1088/0957-4484/23/21/215202

Prezioso, M., Merrikh-Bayat, F., Hoskins, B. D., Adam, G. C., Likharev, K. K., and Strukov, D. B. (2015). Training and Operation of an Integrated Neuromorphic Network Based on Metal-Oxide Memristors. *Nature* 521 (7550), 61–64. doi:10.1038/nature14441

Rahman, M. A., Walia, S., Naznee, S., Taha, M., Nirantar, S., Rahman, F., et al. (2020). Artificial Somatosensors: Feedback Receptors for Electronic Skins. *Adv. Intell. Syst.* 2 (11), 2000094. doi:10.1002/aisy.202000094

Sawa, A. (2008). Resistive Switching in Transition Metal Oxides. *Mater. Today* 11 (6), 28–36. doi:10.1016/s1369-7021(08)70119-6

Scott, J. F., and Paz de Araujo, C. A. (1989). Ferroelectric Memories. *Science* 246 (4936), 1400–1405. doi:10.1126/science.246.4936.1400

Shan, X., Zhao, C., Wang, X., Wang, Z., Fu, S., Lin, Y., et al. (2022). Plasmonic Optoelectronic Memristor Enabling Fully Light-Modulated Synaptic Plasticity for Neuromorphic Vision. *Adv. Sci.* 9 (6), 2104632. doi:10.1002/advs.202104632

Shi, J., Ha, S. D., Zhou, Y., Schoofs, F., and Ramanathan, S. (2013). A Correlated Nickelate Synaptic Transistor. *Nat. Commun.* 4, 2676. doi:10.1038/ncomms3676

Shulaker, M. M., Hills, G., Park, R. S., Howe, R. T., Saraswat, K., Wong, H.-S. P., et al. (2017). Three-dimensional Integration of Nanotechnologies for Computing and Data Storage on a Single Chip. *Nature* 547 (7661), 74–78. doi:10.1038/nature22994

Silver, D., Huang, A., Maddison, C. J., Guez, A., Sifre, L., van den Driessche, G., et al. (2016). Mastering the Game of Go with Deep Neural Networks and Tree Search. *Nature* 529 (7587), 484–489. doi:10.1038/nature16961

Stoliar, P., Tranchant, J., Corraze, B., Janod, E., Besland, M.-P., Tesler, F., et al. (2017). A Leaky-Integrate-And-Fire Neuron Analog Realized with a Mott Insulator. *Adv. Funct. Mat.* 27 (11), 1604740. doi:10.1002/adfm.201604740

Sun, L., Zhang, Y., Hwang, G., Jiang, J., Kim, D., Eshete, Y. A., et al. (2018). Synaptic Computation Enabled by Joule Heating of Single-Layered Semiconductors for Sound Localization. *Nano Lett.* 18 (5), 3229–3234. doi:10.1021/acs.nanolett.8b00994

Sun, Y., Zheng, X., Yan, X., Liao, Q., Liu, S., Zhang, G., et al. (2017). Bioinspired Tribotronic Resistive Switching Memory for Self-Powered Memorizing Mechanical Stimuli. *ACS Appl. Mat. Interfaces* 9 (50), 43822–43829. doi:10.1021/acsami.7b15269

Tan, Z.-H., Yang, R., Terabe, K., Yin, X.-B., Zhang, X.-D., and Guo, X. (2016). Synaptic Metaplasticity Realized in Oxide Memristive Devices. *Adv. Mat.* 28 (2), 377–384. doi:10.1002/adma.201503575

Tee, B. C.-K., Chortos, A., Berndt, A., Nguyen, A. K., Tom, A., McGuire, A., et al. (2015). A Skin-Inspired Organic Digital Mechanoreceptor. *Science* 350 (6258), 313–316. doi:10.1126/science.aaa9306

Theis, T. N., and Wong, H.-S. P. (2017). The End of Moore's Law: A New Beginning for Information Technology. *Comput. Sci. Eng.* 19 (2), 41–50. doi:10.1109/mcse.2017.29

Torrezan, A. C., Strachan, J. P., Medeiros-Ribeiro, G., and Williams, R. S. (2011). Sub-nanosecond Switching of a Tantalum Oxide Memristor. *Nanotechnology* 22 (48), 485203. doi:10.1088/0957-4484/22/48/485203

Tsuruoka, T., Hasegawa, T., Terabe, K., and Aono, M. (2012). Conductance Quantization and Synaptic Behavior in a Ta2O5-Based Atomic Switch. *Nanotechnology* 23 (43), 435705. doi:10.1088/0957-4484/23/43/435705

Tuma, T., Pantazi, A., Le Gallo, M., Sebastian, A., and Eleftheriou, E. (2016). Stochastic Phase-Change Neurons. *Nat. Nanotech* 11 (8), 693–699. doi:10.1038/nnano.2016.70

Vidiš, M., Plecenik, T., Moško, M., Tomašec, S., Roch, T., Satrapinskyy, L., et al. (2019). Gasistor: A Memristor Based Gas-Triggered Switch and Gas Sensor with Memory. *Appl. Phys. Lett.* 115 (9), 093504. doi:10.1063/1.5099685

Vinyals, O., Babuschkin, I., Czarnecki, W. M., Mathieu, M., Dudzik, A., Chung, J., et al. (2019). Grandmaster Level in StarCraft II Using Multi-Agent Reinforcement Learning. *Nature* 575 (7782), 350–354. doi:10.1038/s41586-019-1724-z

Wan, C., Chen, G., Fu, Y., Wang, M., Matsuhisa, N., Pan, S., et al. (2018). An Artificial Sensory Neuron with Tactile Perceptual Learning. *Adv. Mat.* 30 (30), 1801291. doi:10.1002/adma.201801291

Wan, C. J., Zhu, L. Q., Zhou, J. M., Shi, Y., and Wan, Q. (2014). Inorganic Proton Conducting Electrolyte Coupled Oxide-Based Dendritic Transistors for Synaptic Electronics. *Nanoscale* 6 (9), 4491–4497. doi:10.1039/c3nr05882d

Wan, Q., Zeng, F., Sun, Y., Chen, T., Yu, J., Wu, H., et al. (2022). Memristive Behaviors Dominated by Reversible Nucleation Dynamics of Phase-Change Nanoclusters. *Small* 18, 2105070. doi:10.1002/smll.202105070

Wang, H., Zhao, Q., Ni, Z., Li, Q., Liu, H., Yang, Y., et al. (2018a). A Ferroelectric/Electrochemical Modulated Organic Synapse for Ultraflexible, Artificial Visual-Perception System. *Adv. Mat.* 30 (46), 1803961. doi:10.1002/adma.201803961

Wang, J., Wang, C., Cai, P., Luo, Y., Cui, Z., Loh, X. J., et al. (2021). Artificial Sense Technology: Emulating and Extending Biological Senses. *ACS Nano* 15 (12), 18671–18678. doi:10.1021/acsnano.1c10313

Wang, M., Cai, S., Pan, C., Wang, C., Lian, X., Zhuo, Y., et al. (2018). Robust Memristors Based on Layered Two-Dimensional Materials. *Nat. Electron* 1 (2), 130–136. doi:10.1038/s41928-018-0021-4

Wang, M., Luo, Y., Wang, T., Wan, C., Pan, L., Pan, S., et al. (2021). Artificial Skin Perception. *Adv. Mat.* 33 (19), 2003014. doi:10.1002/adma.202003014

Wang, Q., Niu, G., Ren, W., Wang, R., Chen, X., Li, X., et al. (2021). Phase Change Random Access Memory for Neuro-Inspired Computing. *Adv. Electron. Mat.* 7 (6), 2001241. doi:10.1002/aelm.202001241

Wang, T.-Y., Meng, J.-L., Li, Q.-X., He, Z.-Y., Zhu, H., Ji, L., et al. (2021). Reconfigurable Optoelectronic Memristor for In-Sensor Computing Applications. *Nano Energy* 89, 106291. doi:10.1016/j.nanoen.2021.106291

Wang, T., Huang, H. M., Wang, X. X., and Guo, X. (2021). An Artificial Olfactory Inference System Based on Memristive Devices. *InfoMat* 3 (7), 804–813. doi:10.1002/inf2.12196

Wang, W., Pedretti, G., Milo, V., Carboni, R., Calderoni, A., Ramaswamy, N., et al. (2018c). Learning of Spatiotemporal Patterns in a Spiking Neural Network with Resistive Switching Synapses. *Sci. Adv.* 4 (9), eaat4752. doi:10.1126/sciadv.aat4752

Wang, X., Fang, Z., Li, X., Chen, B., Gao, B., Kang, J., et al. (2012a2012). Highly Compact 1T-1R Architecture (4F 2 Footprint) Involving Fully CMOS Compatible Vertical GAA Nano-Pillar Transistors and Oxide-Based RRAM Cells Exhibiting Excellent NVM Properties and Ultra-low Power Operation. *Int. Electron Devices Meet.* 2026, 21–20.26. 24.()

Wang, Z., Hong, Q., and Wang, X. (2019). Memristive Circuit Design of Emotional Generation and Evolution Based on Skin-like Sensory Processor. *IEEE Trans. Biomed. Circuits Syst.* 13 (4), 631–644. doi:10.1109/TBCAS.2019.2923055

Wang, Z. Q., Xu, H. Y., Li, X. H., Yu, H., Liu, Y. C., and Zhu, X. J. (2012b). Synaptic Learning and Memory Functions Achieved Using Oxygen Ion Migration/Diffusion in an Amorphous InGaZnO Memristor. *Adv. Funct. Mat.* 22 (13), 2759–2765. doi:10.1002/adfm.201103148

Wang, Z., Rao, M., Han, J.-W., Zhang, J., Lin, P., Li, Y., et al. (2018d). Capacitive Neural Network with Neuro-Transistors. *Nat. Commun.* 9 (1), 3208. doi:10.1038/s41467-018-05677-5

Waser, R. (2009). Resistive Non-volatile Memory Devices (Invited Paper). *Microelectron. Eng.* 86 (7-9), 1925–1928. doi:10.1016/j.mee.2009.03.132

Wen, C., Hong, J., Ru, F., Li, Y., and Quan, S. (2019). A Novel Memristor-Based Gas Cumulative Flow Sensor. *IEEE Trans. Ind. Electron.* 66 (12), 9531–9538. doi:10.1109/tie.2019.2891436

Wong, H.-S. P., Lee, H.-Y., Yu, S., Chen, Y.-S., Wu, Y., Chen, P.-S., et al. (2012). Metal-Oxide RRAM. *Proc. IEEE* 100 (6), 1951–1970. doi:10.1109/jproc.2012.2190369

Wong, H.-S. P., Raoux, S., Kim, S., Liang, J., Reifenberg, J. P., Rajendran, B., et al. (2010). Phase Change Memory. *Proc. IEEE* 98 (12), 2201–2227. doi:10.1109/jproc.2010.2070050

Wright, L. G., Onodera, T., Stein, M. M., Wang, T., Schachter, D. T., Hu, Z., et al. (2022). Deep Physical Neural Networks Trained with Backpropagation. *Nature* 601 (7894), 549–555. doi:10.1038/s41586-021-04223-6

Wu, Q., Dang, B., Lu, C., Xu, G., Yang, G., Wang, J., et al. (2020). Spike Encoding with Optic Sensory Neurons Enable a Pulse Coupled Neural Network for Ultraviolet Image Segmentation. *Nano Lett.* 20 (11), 8015–8023. doi:10.1021/acs.nanolett.0c02892

Wu, X., Dang, B., Wang, H., Wu, X., and Yang, Y. (2021). Spike-Enabled Audio Learning in Multilevel Synaptic Memristor Array-Based Spiking Neural Network. *Adv. Intell. Syst.* 4 (3), 2100151. doi:10.1002/aisy.202100151

Wu, Z., Lu, J., Shi, T., Zhao, X., Zhang, X., Yang, Y., et al. (2020). A Habituation Sensory Nervous System with Memristors. *Adv. Mat.* 32 (46), 2004398. doi:10.1002/adma.202004398

Xia, Q., and Yang, J. J. (2019). Memristive Crossbar Arrays for Brain-Inspired Computing. *Nat. Mat.* 18 (4), 309–323. doi:10.1038/s41563-019-0291-x

Xu, W., Lee, Y., Min, S.-Y., Park, C., and Lee, T.-W. (2016). Simple, Inexpensive, and Rapid Approach to Fabricate Cross-Shaped Memristors Using an Inorganic-Nanowire-Digital-Alignment Technique and a One-step Reduction Process. *Adv. Mat.* 28 (3), 527–532. doi:10.1002/adma.201503153

Xue, J., Zhu, Z., Xu, X., Gu, Y., Wang, S., Xu, L., et al. (2018). Narrowband Perovskite Photodetector-Based Image Array for Potential Application in Artificial Vision. *Nano Lett.* 18 (12), 7628–7634. doi:10.1021/acs.nanolett.8b03209

Yang, F., Gordon, M. P., and Urban, J. J. (2019). Theoretical Framework of the Thermal Memristor via a Solid-State Phase Change Material. *J. Appl. Phys.* 125 (2), 025109. doi:10.1063/1.5063737

Yang, J. J., Strukov, D. B., and Stewart, D. R. (2013). Memristive Devices for Computing. *Nat. Nanotech* 8 (1), 13–24. doi:10.1038/nnano.2012.240

Yao, P., Wu, H., Gao, B., Eryilmaz, S. B., Huang, X., Zhang, W., et al. (2017). Face Classification Using Electronic Synapses. *Nat. Commun.* 8, 15199. doi:10.1038/ncomms15199

Yao, P., Wu, H., Gao, B., Tang, J., Zhang, Q., Zhang, W., et al. (2020). Fully Hardware-Implemented Memristor Convolutional Neural Network. *Nature* 577 (7792), 641–646. doi:10.1038/s41586-020-1942-4

Yu, T., He, F., Zhao, J., Zhou, Z., Chang, J., Chen, J., et al. (2020). Hf0.5Zr0.5O2-based Ferroelectric Memristor with Multilevel Storage Potential and Artificial Synaptic Plasticity. *Sci. China Mat.* 64 (3), 727–738. doi:10.1007/s40843-020-1444-1

Zang, Y., Shen, H., Huang, D., Di, C.-A., and Zhu, D. (2017). A Dual-Organic-Transistor-Based Tactile-Perception System with Signal-Processing Functionality. *Adv. Mat.* 29 (18), 1606088. doi:10.1002/adma.201606088

Zhang, C., Ye, W. B., Zhou, K., Chen, H. Y., Yang, J. Q., Ding, G., et al. (2019). Bioinspired Artificial Sensory Nerve Based on Nafion Memristor. *Adv. Funct. Mat.* 29 (20), 1808783. doi:10.1002/adfm.201808783

Zhang, S.-R., Zhou, L., Mao, J.-Y., Ren, Y., Yang, J.-Q., Yang, G.-H., et al. (2019). Artificial Synapse Emulated by Charge Trapping-Based Resistive Switching Device. *Adv. Mat. Technol.* 4 (2), 1800342. doi:10.1002/admt.201800342

Zhang, W., Mazzarello, R., Wuttig, M., and Ma, E. (2019). Designing Crystallization in Phase-Change Materials for Universal Memory and Neuro-Inspired Computing. *Nat. Rev. Mater* 4 (3), 150–168. doi:10.1038/s41578-018-0076-x

Zhang, X., Liu, S., Zhao, X., Wu, F., Wu, Q., Wang, W., et al. (2017). Emulating Short-Term and Long-Term Plasticity of Bio-Synapse Based on Cu/a-Si/Pt Memristor. *IEEE Electron Device Lett.* 38 (9), 1208–1211. doi:10.1109/led.2017.2722463

Zhu, L. Q., Wan, C. J., Guo, L. Q., Shi, Y., and Wan, Q. (2014). Artificial Synapse Network on Inorganic Proton Conductor for Neuromorphic Systems. *Nat. Commun.* 5, 3158. doi:10.1038/ncomms4158

Zucker, R. S., and Regehr, W. G. (2002). Short-term Synaptic Plasticity. *Annu. Rev. Physiol.* 64, 355–405. doi:10.1146/annurev.physiol.64.092501.114547

Conflict of Interest: The authors declare that the research was conducted in the absence of any commercial or financial relationships that could be construed as a potential conflict of interest.